Seasonal and multi-annual variation in the abundance of isoprenoid GDGT membrane lipids and their producers in the water column of a meromictic equatorial crater lake (Lake Chala, East Africa)

A.J. Baxter [a], [*], [1], L.G.J. van Bree [a], [1], F. Peterse [a], E.C. Hopmans [b], L. Villanueva [a], [b], D. Verschuren [c], J.S. Sinninghe Damsté [a], [b]

[a] Utrecht University, Faculty of Geosciences, Department of Earth Sciences, Princetonlaan 8A, 3584 CB, Utrecht, the Netherlands
[b] NIOZ Royal Netherlands Institute for Sea Research, Department of Marine Microbiology and Biogeochemistry, PO Box 59, 1790 AB, Den Burg, the Netherlands
[c] Ghent University, Limnology Unit, K.L. Ledeganckstraat 35, B-9000, Gent, Belgium

ABSTRACT

Isoprenoid glycerol dialkyl glycerol tetraethers (isoGDGTs) are membrane lipids of Archaea. Organic biomarker proxies associated with these lipids, such as the TEX$_{86}$ paleothermometer and Branched and Isoprenoid Tetraether (BIT) index, are often used in paleoenvironmental reconstructions for the marine environment, but their general applicability in lacustrine settings is hampered by limited understanding of the biological sources and environmental drivers influencing isoGDGT production. To validate the use of isoGDGT proxies in lakes, we studied the occurrence of isoGDGTs in Lake Chala, a permanently stratified (meromictic) crater lake in equatorial East Africa. We analyzed the abundance and distribution of isoGDGTs in 17 depth profiles of suspended particulate matter (SPM) collected monthly between September 2013 and January 2015, and compared this with the abundance and composition of archaea based on 16S rRNA gene and quantitative PCR analysis. Both isoGDGTs and archaeal abundance in the SPM were exceptionally low throughout the study period. In the oxygenated part of the water column, higher fractional abundances of crenarchaeol are matched by a predominance of the ammonia-oxidizing Thaumarchaeota I.1b that are known to produce this GDGT, whereas deep anoxic water layers are characterized by high fractional abundances of GDGT-0 as well as the anaerobic heterotrophic Group C3 MCG Bathyarchaea and specific euryarchaeotal methanogens. Analysis of intact polar lipid (IPL) isoGDGTs using SPM depth profiles from three months representing distinct seasons during the study period revealed the presence of several IPLs of GDGT-0 in the anoxic lower water column, which are rarely found in natural settings. IPL GDGT-0 with a phosphatidylglycerol (PG-), monohexose-phosphatidylglycerol (MH-PG-) and dihexose-phosphatidylglycerol (DH-PG-) head-group was typically only present just above the lake bottom at 90 m depth and probably reflect specific communities of anaerobic archaea. We also determined the flux and distribution of isoGDGTs in settling particles collected monthly between November 2006 and January 2015 from a sediment trap suspended at 35 m water depth to assess seasonal and inter-annual variability in surface-water isoGDGT production, and compared this with the temporal distribution of isoGDGTs in the 25,000-year long sediment record from Lake Chala. Monthly variation of isoGDGTs in the 98-month settling-particles record did not show a strong annual pattern related to seasonal water-column mixing and stratification, likely because the oxycline was regularly situated below sediment-trap depth. Episodes of high GDGT-0 concentrations relative to crenarchaeol in the settling particles can therefore be linked to periods of exceptionally shallow oxycline depth, which suppresses the thaumarchaeotal bloom. During such intervals, TEX$_{86}$-based paleotemperatures are not reliable because isoGDGT input from other archaeal sources disproportionally influences TEX$_{86}$ values and creates a cold-temperature bias. Additionally, the abundance of the crenarchaeol isomer relative to crenarchaeol (f[CREN']) gradually increases during such episodes of high GDGT-0/crenarchaeol ratio, suggesting increasing dominance of Group I.1b over Group I.1a Thaumarchaeota, and might prove a good marker for prolonged shallow-oxycline conditions. Most

---

* Corresponding author.
  E-mail address: A.J.Baxter@uu.nl (A.J. Baxter).
[1] These authors contributed equally.

importantly, the associated near-absence of crenarchaeol during times of strong upper-water-column stratification results in high BIT-index values. We propose that this suppression mechanism may be the principal driver of BIT-index variation in the sediment record of Lake Chala, and the main source of observed congruence between the BIT index and climate-driven lake-level variation on long time scales.

1. Introduction

Lipid biomarkers in lake sediments are increasingly used to reconstruct past environmental changes such as temperature, rainfall and vegetation dynamics in the lake's catchment (e.g., Castañeda and Schouten, 2011; Schouten et al., 2013; Berke, 2018). The sediment records of permanently stratified (meromictic) lakes are especially suitable for such biomarker studies, because the preservation of organic compounds is greatly improved by stable anoxic conditions at the sediment-water interface. Isoprenoid and branched glycerol dialkyl glycerol tetraethers (isoGDGTs and brGDGTs, respectively) represent important groups of sedimentary biomarkers. IsoGDGTs are membrane lipids of Archaea, which biosynthesize varying proportions of isoGDGTs with 0−8 cyclopentyl moieties (GDGT-0 to 8; De Rosa and Gambacorta, 1988), as well as an isoGDGT with 4 cyclopentyl and 1 cyclohexyl moiety called crenarchaeol (Sinninghe Damsté et al., 2002; Holzheimer et al., 2021; structures in Supplementary Fig. S1). GDGT-0 is the most common isoGDGT in Archaea, and is found in chemolithotrophic, ammonia-oxidizing Thaumarchaeota (e.g., Sinninghe Damsté et al., 2012b; Schouten et al., 2013; Elling et al., 2017; Bale et al., 2019b), anaerobic methane-oxidizing archaea (e.g., Pancost et al., 2001; Schouten et al., 2001) and methanogenic Euryarchaeota (Schouten et al., 2013, and references therein). GDGT-1 to −3 are common lipids in eury-, cren- and thaumarchaeotal membranes (Schouten et al., 2013, and references therein), whereas crenarchaeol and its isomer have only been found in Thaumarchaeota cultures (e.g., Sinninghe Damsté et al., 2002, 2018; Schouten et al., 2013; Elling et al., 2017; Bale et al., 2019b).

Empirical correlation between the distribution of isoGDGTs in marine surface sediments and local sea surface temperature (SST) led to development of the TetraEther indeX of 86 carbon atoms (TEX$_{86}$; e.g., Schouten et al., 2002; Kim et al., 2010), although it was shown to reflect subsurface temperature at specific locations (e.g. Huguet et al., 2007). TEX$_{86}$ is now widely used as SST proxy in paleoclimate reconstructions. An exploratory study on lakes indicated that the TEX$_{86}$ of lacustrine sediments also reflected lake surface temperature (LST; Powers et al., 2010), although this calibration was based on a substantially smaller number of sites than that for the marine environment. However, the applicability of this paleotemperature proxy in lakes appeared complicated by various confounding factors such as potential input from soil-derived isoGDGTs, or contributions of isoGDGTs produced by methanotrophs, methanogens and other archaea (Blaga et al., 2009, 2011; Powers et al., 2010; Sinninghe Damsté et al., 2012a).

The contribution of isoGDGTs from methanogens can be assessed by the ratio between GDGT-0 and crenarchaeol. A ratio of >2 indicates that methanogens, which also produce GDGT-0, contribute substantially to the total sedimentary isoGDGT pool (e.g., Blaga et al., 2009; Bechtel et al., 2010), in which case the TEX$_{86}$ proxy cannot be used. Despite these uncertainties, the TEX$_{86}$ paleothermometer has produced several important records of past LST variation (e.g., Powers et al., 2005, 2011; Tierney et al., 2008; Woltering et al., 2011; Blaga et al., 2013; Sun et al., 2020), mainly from large lakes.

To assess the input of terrestrial material into aquatic environments the Branched and Isoprenoid Tetraether index (BIT index; Hopmans et al., 2004) was developed, in which the relative abundance of soil-derived brGDGTs compared to that of the aquatic isoGDGT crenarchaeol represents the contribution of soil-derived material delivered to the system by erosion and runoff. It was also applied as such to a 25-kyr long sediment core from Lake Chala, a permanently stratified crater lake in equatorial East Africa, where intervals with high BIT-index values were inferred to represent episodes of increased precipitation (Verschuren et al., 2009). However, in following years several studies showed that brGDGTs are also produced within lakes (e.g., Sinninghe Damsté et al., 2009; Tierney et al., 2010; Woltering et al., 2012; Weber et al., 2015, 2018), challenging the initial interpretation of this proxy in lake settings. Therefore, Sinninghe Damsté et al. (2012a) proposed an alternative explanation for the (indirect) relationship between the BIT index and precipitation in Lake Chala, arguing that strong wind and low rainfall promote deep water-column mixing and thus stimulate the internal nutrient cycling supporting primary production and subsequent increase in ammonia. This would allow proliferation of the nitrifying Thaumarchaeota that produce crenarchaeol. On long time scales, conditions of low lake level under dry climate conditions would therefore be associated with greater crenarchaeol production and lower BIT-index values. Conversely, high BIT-index values may be linked to episodic events of intense rainfall, during which strong soil erosion enhances external nutrient input and ammonia levels to the extent that nitrifying Thaumarchaeota are outcompeted by a bloom of nitrifying bacteria (Buckles et al., 2016).

More recently, a detailed study of the water column of Lake Chala confirmed that brGDGTs are produced *in situ* and are mainly restricted to the lower water column, where their distribution is strongly influenced by the depth of seasonal mixing (van Bree et al., 2020). Namely, brGDGTs occur higher up in the water column during periods of strong water-column stratification associated with the rainy seasons, and are restricted to greater depths during periods of deep water-column mixing, suggesting that the bacterial species producing these lipids (Weijers et al., 2006) prefer anoxic conditions. This expansion of the brGDGT producers' niche under conditions of strong water-column stratification may partly explain the positive relationship between the BIT index in Lake Chala and past rainfall variation. On the other hand, it has been shown that variation in the BIT index is more strongly driven by changes in the abundance of crenarchaeol, and less by changes in brGDGT abundance (Sinninghe Damsté et al., 2012a; Buckles et al., 2014, 2016).

The occurrence and distribution of isoGDGTs in Lake Chala have previously been analyzed in a one-year study of monthly-collected settling particles (Sinninghe Damsté et al., 2009). This indicated that isoGDGTs were primarily produced in January and February, i.e. just after the short rain season. The resulting TEX$_{86}$ values failed to capture seasonal temperature variation, but generally did reflect mean annual LST (Sinninghe Damsté et al., 2009). However, production of isoGDGTs (especially GDGT-2) in deeper waters or in the sediment appeared to alter the isoGDGT signature in such a way that the TEX$_{86}$ proxy did not yield reliable results for the Holocene portion of the Lake Chala sediment sequence (Sinninghe Damsté

et al., 2009, 2012a). To identify the potential producers of isoGDGTs in Lake Chala, the depth distribution of different isoGDGTs was compared with those of archaeal 16S rRNA sequences in suspended particulate matter (SPM) collected in two months with contrasting water-column conditions, namely deep mixing in September 2006 (Sinninghe Damsté et al., 2009) versus stratification in February 2010 (Buckles et al., 2013). During the deep-mixing season, isoGDGTs were most abundant between 50 and 90 m depth, whereas crenarchaeol also showed modestly increased concentrations at 15 and 30 m depth (Sinninghe Damsté et al., 2009).

Extractable isoGDGTs can be divided into core lipids (CL) and intact polar lipids (IPL; membrane lipids which have retained their head groups). As IPL GDGTs in lake sediments have presumably been produced by 'living' microbes, they are often studied in comparison to the corresponding 'fossil' core lipids. An increasingly diverse group of IPL GDGTs are being discovered in natural settings, providing important insights into both lipid preservation and potential producers (e.g. Tierney et al., 2012; Buckles et al., 2014; Bale et al., 2019a,b). Under stratified conditions in Lake Chala, the concentrations of IPL and CL crenarchaeol and all other isoGDGTs peaked at 40 m depth (Buckles et al., 2013), except IPL GDGT-0 of which the concentration peaked in deep anoxic water. Based on 16S rRNA gene analysis this active production of crenarchaeol in the oxygenated upper water column of Lake Chala was attributed to Thaumarchaeota of Group I.1a and I.1b (the latter also known as the Soil Crenarchaeotic Group; SCG; Pester et al., 2011 and references therein). This was in good agreement with the composition of the polar head groups of the IPL crenarchaeol, which is similar to that of cultivated Thaumarchaeota (Buckles et al., 2013). The high concentration of GDGT-0 in the anoxic deep water was linked to non-methanotrophic archaea of Group C3 (Sinninghe Damsté et al., 2009; Buckles et al., 2013), formerly known as Crenarchaeota Group 1.2 but currently classified as 'Miscellaneous Crenarchaeotic Group' (MCG), a subgroup of the phylum Bathyarchaeota (Kubo et al., 2012; Lavergne et al., 2018). The presence of archaeal groups other than Thaumarchaeota that can also synthesize isoGDGTs has obvious consequences for the reliability of isoGDGT-based paleoenvironmental proxies in Lake Chala, and possibly, all lakes (Buckles et al., 2013).

The initial findings on isoGDGT depth distribution and sources in Lake Chala summarized above were based on 'snapshot' views of its water column. Considering that sediment-trap and high-resolution sedimentary time series reveal large inter-annual variability in isoGDGT flux and distribution (Sinninghe Damsté et al., 2009; Buckles et al., 2014, 2016), this may also be the case for their archaeal sources. Therefore, the present study aims to further investigate spatio-temporal patterns in the production and distribution of isoGDGTs and their producers in Lake Chala. This is accomplished by analyzing the distribution and abundance of CL + IPL isoGDGTs and archaeal 16S rRNA gene copies in SPM depth profiles collected at monthly intervals over a 17-month period. Additionally, we analyzed the IPL GDGTs in the SPM profiles from December 2013, April 2014 and September 2014, representing distinct seasons. Finally, we looked for recurrent patterns in the 98-month record of settling particles from the sediment trap suspended in Lake Chala in order to link seasonal and multi-annual trends in isoGDGT production within the upper water column to potential environmental drivers. The principal and ultimate objective of these combined analyses is to better constrain the interpretation of isoGDGT-based paleoenvironmental proxies, such as the BIT index and TE_{86}, in this and other lakes' sedimentary records.

2. Material and methods

2.1. Study site

Lake Chala (locally known as 'Challa', after a nearby village) is a small (4.2 km²), deep (~90 m) and permanently stratified (meromictic) crater lake, situated at ~880 m above sea level on the border between Kenya and Tanzania (3°19′S, 37°42′E) in the southeastern foothills of Mt. Kilimanjaro. Mean monthly air temperature (MMAT) is highest in January–February (25–27 °C) during the southern hemisphere (SH) summer, and lowest in July–August (20–21 °C). Part of the lake's water budget is maintained by rainfall on the lake surface and inside the steep-sloping crater basin; only occasionally after high rainfall a small creek is activated, which breaches the north-western crater rim (Buckles et al., 2014, Fig. 1). As lake-surface evaporation (1700 mm yr⁻¹) greatly exceeds mean annual rainfall (600 mm yr⁻¹), the lake's water budget must be maintained by a substantial subsurface inflow (Payne, 1970) of water originating from the percolation of rainfall on or above the forest belt on Mt. Kilimanjaro (Hemp, 2006; Bodé et al., 2020).

The tropical rain belt associated with latitudinal migration of the Inter-Tropical Convergence Zone (ITCZ) passes over the region twice yearly, resulting in two wet seasons and two dry seasons. Short rains occur from late October to December, and long rains from March to May. The main dry season occurs during the SH winter from June until September and is characterized by lower air temperature and higher wind speeds. Together these drive turbulent and convective deep mixing of the lake's water column down to 40–60 m depth, while the lower water column remains permanently stratified and anoxic (Wolff et al., 2011; Buckles et al., 2014). Periods of deep mixing (DM) generally start at the end of May, and end in the first half of September (van Bree et al., 2018). During DM, oxygen is injected into progressively deeper water, and phytoplankton productivity increases as nutrient-rich deep water is mixed upwards into the normally unproductive epilimnion (Wolff et al., 2014; van Bree et al., 2018). Conditions of water-column stratification generally develop from September to May, and are
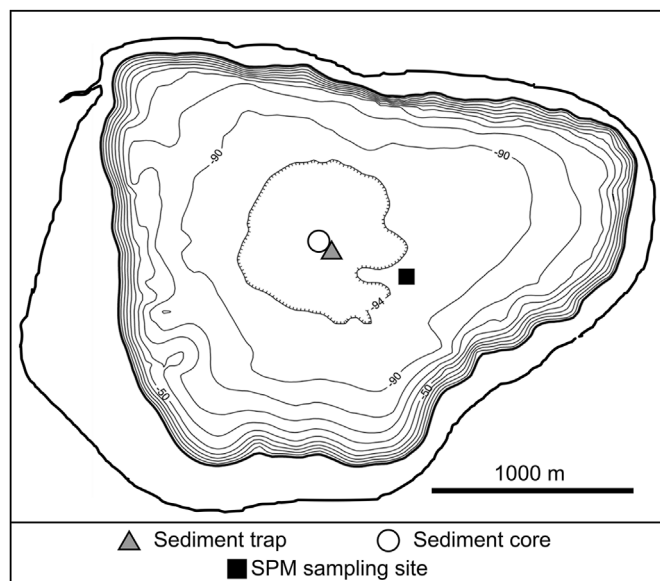
Fig. 1. Bathymetry of Lake Chala relative to its 2003 shoreline with depth contours at 10-m intervals (modified after Moernaut et al., 2010) with sampling locations of suspended particulate matter (SPM; black square), settling particles (sediment trap; grey triangle) and the 25-kyr sediment record (open circle). The outer bold line is the crater rim, confining the catchment area.

strongest during the SH summer months (Wolff et al., 2014; van Bree et al., 2018, 2020). Superimposed on this long period of stratification, shallow mixing (SM) to ~20−25 m depth occurs during the short dry season in between the two rain seasons, when winds are also strong but high surface-water temperature hampers deep mixing. The timing of this SM is variable, but generally starts between the beginning of December and mid-January, and ends between mid-February and mid-March.

2.2. Sample collection

2.2.1. Physical and chemical water-column monitoring

Physical-property profiles of the upper 50 m of the water column of Lake Chala were measured monthly from September 2013 until January 2015, by registering ambient temperature, dissolved oxygen (DO), conductivity (K25) and pH at 1 m (0−24 m) and 2 m (24−50 m) depth intervals with a Hydrolab Quanta® multiprobe on the same day as the collection of water samples for SPM analysis (van Bree et al., 2018). Here we use these data only to trace the depth of the oxycline over this 17-month period, defined as the depth where DO concentration falls below 0.2 mg/L (van Bree et al., 2020). Water samples for CH_4 analysis were collected on 01-11-2016 at the same mid-lake position, using a WildCo® water sampler. From the same 13 water depths selected for SPM sampling (van Bree et al., 2018), 5 L water was brought up as quickly as possible to minimize outgassing. Due to circumstances the sample from 90 m depth was brought up more slowly, consequently this CH_4 measurement had to be dismissed. Two replicate samples each were taken at 50 and 60 m depth. The water was transferred immediately to airtight 12 ml exetainer vials, and stored at room temperature prior to CH_4 analysis. Simultaneously with this water sampling on 01-11-2016, profiles of temperature, conductivity and pH were measured with a Hydrolab Quanta® down to 50 m depth, and extended to 85 m depth using a Hydrolab HL4® multiprobe with sensors calibrated against those of the Quanta instrument. The associated DO profile presented here was measured with the Quanta three weeks later, on 20-11-2016.

2.2.2. Suspended particulate matter

The collection of suspended particulate matter (SPM) for this study was described in detail by van Bree et al. (2018). In short, 5−10 L of lake water was collected at 13 discrete depths between the lake surface and 90 m depth, monthly between September 2013 and January 2015 ($n = 221$). The date of collection was at or near the start of each month as discussed here, with samples collected on, for example, 07-09-2013 representing September 2013, and samples collected on 30-09-2013 representing October 2013 (see Table S1). The samples were filtered on pre-combusted glass fiber GF/F filters (142 mm diameter, Whatman), stored frozen and freeze-dried prior to analysis. For this study we analyzed CL + IPL GDGTs (i.e., including acid-hydrolyzed IPL GDGTs; see section 2.3.2.) in the extracts of SPM from all depths for the months of November 2013 and August 2014, and from 0, 10, 25, 35, 50, 60, 70 and 80 m depth for the 15 other months (total $n = 141$). In addition we analyzed IPL GDGTs in SPM from 20, 30, 45 and 90 m depth collected in December 2013, April 2014 and September 2014 (Table S2).

2.2.3. Settling particles

The collection of settling particles in Lake Chala has been described extensively before (Sinninghe Damsté et al., 2009; Buckles et al., 2014, 2016). In short, in November 2006 a UWITEC® double-funneled sediment trap of 86 mm diameter was installed at 35 m water depth in a mid-lake position (Fig. 1), and emptied and redeployed at approximately monthly intervals during the ensuing

8 years (Table S3). Collected material was allowed to settle for two days, and stored frozen after decantation of excess water. Prior to analysis, the samples were thawed, filtered over pre-weighed and pre-combusted (400 °C, 5h) glass fiber GF/F filters (110 mm diameter, Whatman), frozen and freeze-dried. This study combines new analyses of GDGTs in settling particles representing the period September 2010 to January 2015 ($n = 53$; Table S3), with published data for the period November 2006 to August 2010 (Sinninghe Damsté et al., 2009; Buckles et al., 2014, 2016), also sampled at near-monthly intervals, to cover a total of >8 years ($n = 98$ total samples).

2.3. Sample preparation, extraction and analysis

2.3.1. Methane analysis

To measure CH_4 concentration, a 1 ml high-purity nitrogen (N_2) headspace was generated in the exetainers, after which samples were left to equilibrate for at least 48 h prior to measurement. They were injected by hand on a gas chromatograph flame ionization detector (GC-FID), and measured as technical triplicates. The reported values are the average of these triplicates and their standard deviation. The two pairs of replicate samples at 50 and 60 m yielded similar results.

2.3.2. Analysis of CL GDGTs

Preparation of SPM samples for CL GDGT analysis has been described in detail by van Bree et al. (2018, 2020). In short, the freeze-dried SPM filters were cut in small pieces and extracted using a modified Bligh-Dyer method (Bligh and Dyer, 1959). Each Bligh-Dyer extract was acid-hydrolyzed with 1.5 N hydrochloric acid (HCl) in methanol (MeOH) to release polar head groups from extracted IPLs. Therefore, the GDGTs analyzed in this study represent the total extractable GDGTs (referred to as CL + IPL in the remainder of the text), which is advantageous since IPL GDGTs may form an important fraction of the total GDGT pool (e.g. Buckles et al., 2013; Weber et al., 2017). This hydrolyzed total lipid extract (TLE) was separated on an activated Al_2O_3 column into a apolar, neutral and polar fractions, using hexane:dichloromethane (DCM) (9:1, v:v), DCM, and DCM: MeOH (2:1, v:v) as eluents, respectively. Preparation of the settling-particle samples has also been described elsewhere (Sinninghe Damsté et al., 2009; Buckles et al., 2014; van Bree et al., 2020). In short, the freeze-dried filters with sediment-trap material were cut in small pieces and extracted directly by acid hydrolysis, and the obtained TLE was processed in the same way as the SPM. A known amount of internal standard (99 ng $GDGT_{46}$; Huguet et al., 2006) was added to the polar fractions of the SPM and settling-particle extracts. These fractions were re-dissolved in hexane:isopropanol (99:1, v:v) and passed over a 0.45 μm PTFE filter prior to analysis.

The CL + IPL GDGTs present in the polar fractions were analyzed by ultrahigh-performance liquid chromatography (UHPLC) following the method of Hopmans et al. (2016), using an Agilent 1260 Infinity UHPLC system coupled to an Agilent 6130 single quadrupole mass detector, either at Utrecht University (most SPM) or at the Royal NIOZ (settling particles and SPM at 0 m, except SPM from November 2013 and September 2014). Separation was achieved by two silica Waters Acquity UPLC HEB Hilic (1.7 μm, 2.1 mm × 150 mm) columns at 30 °C, preceded by a guard column with similar packing. Initially isocratic elution was used for GDGT separation, starting with 82% A (hexane) and 18% B (hexane:isopropanol, 9:1, v:v) for 25 min at a flow rate of 0.2 mL min^{-1}, followed by a linear gradient to 70% A and 30% B for 25 min. Injection volume was 10 μL for settling particles, and 20 μL for SPM. Ionization of the GDGTs was achieved by atmospheric-pressure chemical ionization with as source conditions a gas temperature

(N_2) of 200 °C, vaporizer temperature of 400 °C, N_2 flow of 6 L min^{-1}, capillary voltage of 3500 V, nebulizer pressure of 25 psi and corona current of 5.0 μA. GDGTs were identified by detecting the [M+H]$^+$ ions in selected ion monitoring (SIM) mode for m/z 1018.0, 1020.0, 1022.0, 1032.0, 1034.0, 1036.0, 1046.0, 1048.0 and 1050.0 (brGDGTs), m/z 1292.3, 1294.3, 1296.3, 1298.3, 1300.3 and 1302.3 (isoGDGTs), and m/z 743.8 (internal standard) with a mass window of 1.0. Peak area integration of the GDGTs was done with Chemstation (SPM) or Agilent Masshunter (settling particles, SPM at 0 m) software. Individual GDGTs were quantified by comparing their areas to that of the internal C_{46} GTGT (glycerol trialkyl glycerol tetraether) standard, assuming a comparable response of the mass spectrometer for all GDGTs. Selected sediment-trap samples were measured twice in different concentrations ($n = 13$), which yielded comparable fluxes, fractional abundances and index values. For example, the difference between duplicates was typically <8% for total isoGDGT flux, typically <0.07 for TEX$_{86}$, and always <0.013 for the BIT index.

2.3.3. Analysis of IPL GDGTs

IPL GDGTs in SPM samples were extracted from the freeze-dried filters using a modified Bligh Dyer extraction as described in detail by Bale et al. (2021). In short, filters were first extracted twice with a solution of MeOH: DCH: Phosphate-buffer (2:1:0.8, v:v:v) adjusted to a pH of 7–8 with 1 N HCl and then twice using a solution of MeOH: DCM: Trichloroacetic acid (2:1:0.8, v:v:v) adjusted with 2 N KOH to a pH of 2–3. After phase separation, the organic phases of both extracts were combined and dried. After addition of 24 ng of a deuterated betaine lipid (1,2-dipalmitoyl-sn-glycero-3-O-4′-[N,N,N-trimethyl(d9)]-homoserine; Avanti Polar Lipids Inc., Alabaster, AL, USA) as internal standard, each TLE was filtered with a 0.45 μm regenerated cellulose syringe filter (4 mm diameter). TLEs were dissolved in MeOH: DCM (9:1, v:v) prior to injection and analyzed using Ultra High Pressure Liquid Chromatography-High Resolution tandem Mass Spectrometry (UHPLC-HRMS^2) according to the method of Wörmer et al. (2013) with modifications as described by Bale et al. (2019c). Lipids were analyzed within a mass range of m/z 345–2000. We used an Agilent 1290 Infinity I UHPLC equipped with thermostatted auto-injector and column oven, coupled to a Q Exactive Orbitrap MS with Ion Max source with heated electrospray ionization (HESI) probe (Thermo Fisher Scientific, USA).

IPLs were identified based on the calculated exact masses of their protonated, ammoniated and sodiated ions ([M+H]$^+$, [M + NH$_4$]$^+$ and [M+Na]$^+$, respectively) where present and characteristic MS^2 fragmentation patterns (Yoshinaga et al., 2011; Besseling et al., 2018). Peak integrations were performed on summed mass chromatograms (within 5 ppm mass accuracy and with a 5-point gaussian smoothing applied) of all relevant ions and abundant isotopologues (see Table S4 for full list). In case of significant in-source fragmentation, the resulting fragments were also included during peak integration. Peak areas were normalized based on the response of the internal standard to account for ion suppression and variable machine performance. The amount of IPLs is expressed in area units per liter (AU L^{-1}).

2.3.4. DNA extraction, 16S rRNA gene sequencing and analysis, and quantitative PCR of gene sequences

DNA extraction, 16S rRNA gene sequencing and analysis, and quantitative PCR of 16S rRNA gene sequences has been described in detail by van Bree et al. (2020). In short, DNA was extracted from a small section (1/32) of the SPM filters, using the PowerSoil DNA extraction kit (Mo Bio Laboratories, Carlsbad, CA, USA). The 16S rRNA gene amplicon sequencing and analysis was performed with the general 16S rRNA archaeal and bacteria primer pair 515F and

806RB, targeting the V4 region (Caporaso et al., 2012) as described by Besseling et al. (2018). PCR products were gel-purified using the QIAquick Gel-Purification kit (Qiagen), pooled and diluted. Sequencing was performed at the Utrecht Sequencing Facility (Utrecht, the Netherlands) using an Illumina MiSeq 2 × 300 bp sequencing platform. The 16S rRNA gene amplicon sequences were analyzed by the Cascabel pipeline (Abdala Asbun et al., 2020) including quality assessment by FastQC (Andrews, 2010), assembly of the paired-end reads with PEAR (Zhang et al., 2014), and taxonomic assignment (including picking of a representative set of sequences with the 'longest' method; Caporaso et al., 2010) with BLAST (Altschul et al., 1990) by using the Silva 128 release as reference database (https://www.arb-silva.de/). 16S rRNA gene copies were quantified using quantitative PCR (qPCR) with the same primer pair as for amplicon sequencing (515F, 806RB). The qPCR reaction mixture (25 μl) contained 1 U of Pico Maxx high fidelity DNA polymerase (Stratagene, Agilent Technologies, Santa Clara, CA), 2.5 μl of 10x Pico Maxx PCR buffer, 2.5 μl 2.5 mM of each dNTP, 0.5 μl BSA (20 mg ml^{-1}), 0.02 pmol μl^{-1} of primers, 10,000-fold diluted SYBR Green® (Invitrogen) (optimized concentration), 0.5 μl of MgCl$_2$ (50 mM), and ultrapure sterile water. Cycling conditions for the qPCR reaction were the following: initial denaturation at 98 °C for 30s, 45 cycles of 98 °C for 10s, 56 °C for 20s, followed by a plate read, 72 °C of 30s, 80 °C for 25s. Specificity of the reaction was tested with a gradient melting temperature assay, from 55 °C to 95 °C with a 0.5 °C increment each 5 s. The qPCR reactions were performed in triplicate with standard curves from 100 to 107 molecules per microliter. qPCR efficiency for the 16S rRNA quantification was on average 95% with R^2 = 0.998.

2.4. Proxy calculation

Molecular structures of all GDGTs discussed in this study are shown in Figure S1. The BIT index (Hopmans et al., 2004) was modified by De Jonge et al. (2014) to include 6-methyl brGDGT isomers and was calculated as follows:

$$BIT = ([Ia]+[IIa]+[IIa']+[IIIa]+[IIIa']) / ([Ia]+[IIa]+[IIa']+[IIIa]+[IIIa']+[crenarchaeol]) \quad (1)$$

where [x] can represent either the absolute or fractional abundance of GDGT-x. The crenarchaeol isomer (cren') to crenarchaeol ratio was calculated as follows:

$$f[CREN'] = [cren'] / ([cren']+[crenarchaeol]) \quad (2)$$

TEX$_{86}$ was calculated as defined by Schouten et al. (2002):

$$TEX_{86} = ([GDGT\text{-}2]+[GDGT\text{-}3]+[cren']) / ([GDGT\text{-}1]+[GDGT\text{-}2]+[GDGT\text{-}3]+ [cren']) \quad (3)$$

2.5. Statistical analysis

To assign (a) possible source(s) of individual isoGDGTs, isoGDGT concentrations (ng L^{-1}) were correlated with the absolute abundance of archaeal groups as estimated from their number of 16S rRNA gene copies L^{-1}. The latter was calculated by multiplying the relative abundance obtained through 16S rRNA gene amplicon sequencing by the total 16S rRNA gene copies per liter based on qPCR, under the simplifying assumption that all archaeal species present in the lake contain a single 16S rRNA copy in their genome.

3. Results

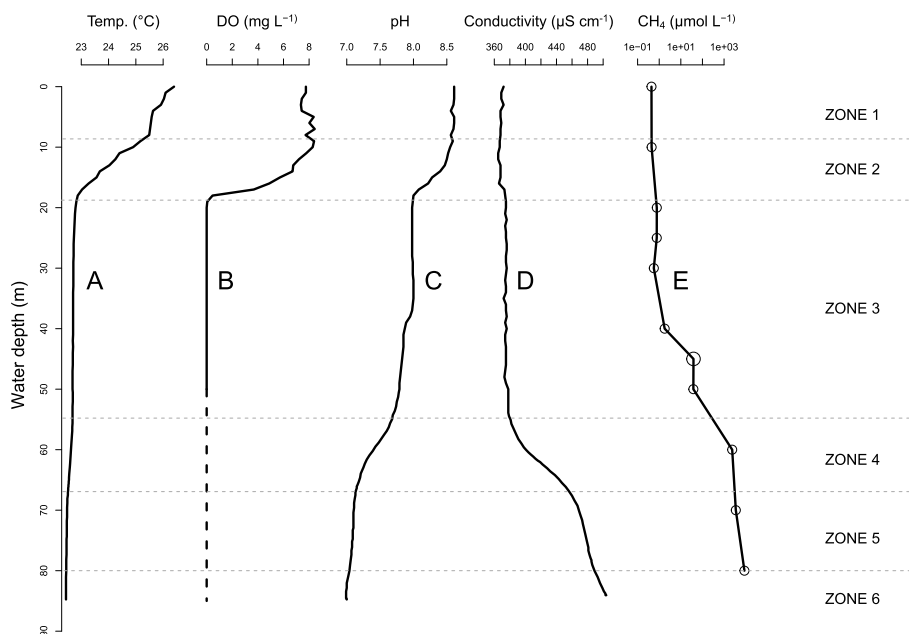## 3.1. Physical and chemical properties of the water column

Physical and chemical water-column properties measured on November 1, 2016 indicate stratified conditions, including a shallow oxycline (~20 m depth) and a strong methane gradient (Fig. 2). Methane concentrations in the water column of Lake Chala increased sharply with depth from 0.44 to 0.77 μmol L^{-1} in the upper 30 m to between 1.8 and 49 μmol L^{-1} at 40−50 m, and reach values of 2400−8800 μmol L^{-1} between 60 and 80 m depth (Fig. 2E). This strong methane gradient is stabilized in time, due to permanent temperature and chemical stratification of the lower water column, here labeled zones 4−6 (Fig. 2A−D), following Buckles et al. (2014). This is in contrast to zones 1−3, the relative thicknesses of which are controlled by wind-driven turbulence, air temperature, and productivity, that vary seasonally and between successive years. We therefore consider this methane profile representative for present-day Lake Chala, even though it was obtained outside of the sampling period for SPM and settling particles.

3.2. CL + IPL isoGDGTs in SPM

All targeted extractable isoGDGTs (GDGT-0 to −3, crenarchaeol and its isomer, cren') were detected in the SPM of Lake Chala (Fig. 3). Again we note that analyzed CL + IPL isoGDGTs represent the sum of CL and hydrolyzed IPL-derived GDGTs. Generally, the summed isoGDGT concentration increased with depth (Fig. 3A), both when the oxycline was located at shallow depth (~15−25 m; September 2013 to March 2014) and when it was located much deeper (>35 m; August to November 2014). GDGT-0 was the only isoGDGT present above detection limit in all SPM samples analyzed ($n = 141$) and often dominant, with a fractional abundance exceeding 0.60 in 95% of the SPM samples. Particularly high

concentrations of GDGT-0 were measured in the lower water column at >50 m depth (up to 112 ng L^{-1} at 80 m in November 2014; average concentration 12 ng L^{-1}; Fig. 3C). IsoGDGTs-1, -2, -3 and crenarchaeol occurred less frequently and in much lower concentrations than GDGT-0 (Fig. 3B; D). Crenarchaeol was present in ~70% of all samples (average concentration 0.1 ng L^{-1} with a maximum of 3.2 ng L^{-1}), followed by GDGT-1 (60%; max. 0.9 ng L^{-1}), cren' (41%; max. 0.2 ng L^{-1}), GDGT-2 (38%, max. 0.4 ng L^{-1}) and GDGT-3 (6%, max. 0.05 ng L^{-1}). The spatio-temporal distribution of crenarchaeol and the sum of GDGT-1, -2 and -3 showed some similarity (Fig. 3B; D), both reaching highest concentrations at 60 m depth in August 2014. GDGT-1 showed an additional maximum at 50 m depth between May and September 2014, i.e. during the period of deep water-column mixing. Concentrations of GDGT-0 and crenarchaeol are not correlated ($r = 0.02$, $p = 0.84$, $n = 103$). Correlations among the other isoGDGTs were not calculated due to the high number of samples where these compounds were below detection limit.

Although crenarchaeol concentrations in Lake Chala SPM were low overall, its fractional abundance was generally highest in the upper water column (max. 0.53, at 25 m in December 2014; Table S1), mostly due to the relatively low concentrations of GDGT-0 there (Fig. 3C). Peaks in crenarchaeol abundance were few, and restricted to narrow depth ranges that varied over the seasons. For example, in the well-resolved SPM profile of November 2013 a modest crenarchaeol peak occurs at 25 m depth (1.4 ng L^{-1}), and two smaller ones at 50 (0.5 ng L^{-1}) and 80 m (0.4 ng L^{-1}), whereas in the profile from August 2014 (actually 31 July) the main peak in crenarchaeol is located at 60 m (3.2 ng L^{-1}), with smaller peaks at 20 (0.6 ng L^{-1}) and 80 m (0.3 ng L^{-1}) (Fig. 3D). In ~27% of the measured SPM samples crenarchaeol was below detection limit, consequently the BIT index of these samples is 1.00 and the GDGT-0/crenarchaeol ratio limitless (Table S1). Overall, the BIT index in this SPM dataset ranges from 0.56 to 1.00 (Fig. S2A). On average, reliable GDGT-0/crenarchaeol values were lowest at the lake surface (0 m: range 1.66−5.54; mean = 3.12) and increased with depth

Fig. 2. Physical and chemical properties of the water column of Lake Chala on 01-11-2016: temperature (A; in °C); dissolved oxygen (DO) concentration (B; in mg L^{-1}), pH (C), conductivity (D; K25 in μS cm^{-1} at 25 °C) as proxy for the concentration of dissolved solids, and methane concentration (E; in μmol L^{-1}, note the logarithmic scale). Error bars of the duplicate or triplicate methane concentration measurements at each depth are within the size of each dot. Following Buckles et al. (2014) the water column is divided from top to bottom in six zones, of which the boundaries are defined on the basis of changing physical and chemical properties. Zone 1 mixes daily, zones 2−3 at least once annually, zones 4−6 are permanently stratified (i.e., they mix at frequencies distinctly less than annually); see text for details.
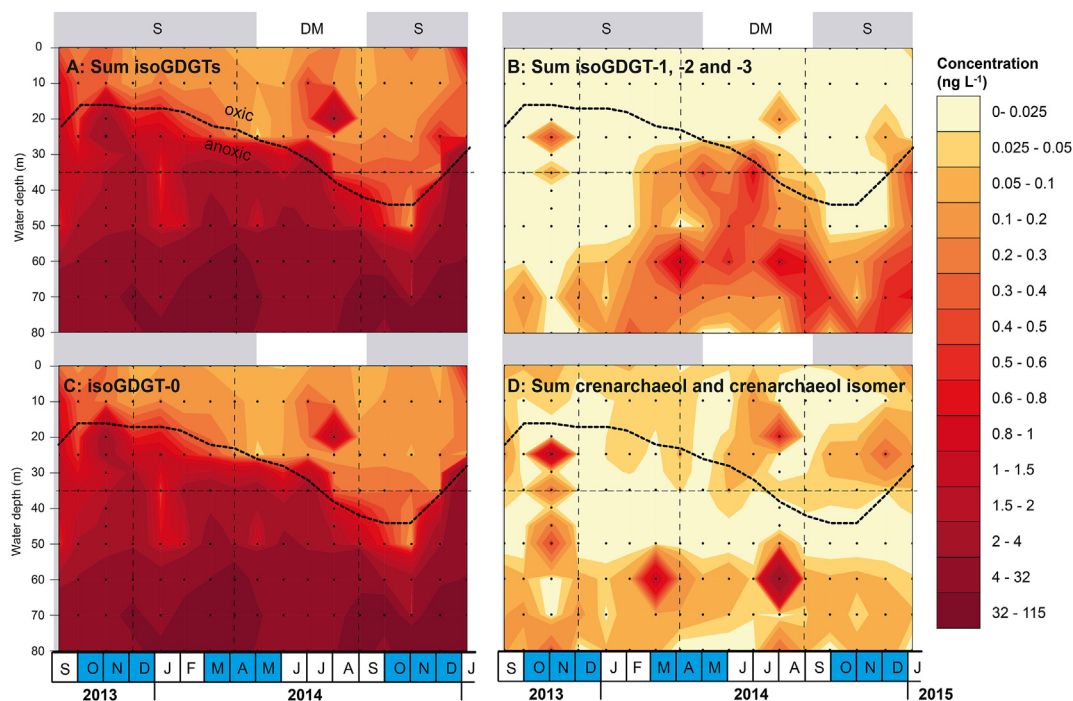
Fig. 3. Interpolated concentrations of isoGDGTs (in ng L^{-1}) in SPM from Lake Chala sampled at approximately monthly intervals between September 2013 and January 2015. Concentrations of total isoGDGTs (A), sum of isoGDGTs-1, -2, and -3 (B), GDGT-0 (C), and sum of crenarchaeol and its isomer (D). The varying position of the oxic-anoxic boundary (oxycline, or depth to anoxia; van Bree et al., 2020), the static position of the sediment trap (thin dashed line at 35 m depth), and the SPM sampling grid (black dots) are indicated. Vertical dashed lines indicate the three months for which IPL GDGTs were also analyzed. The grey background shading shows the seasonal periods of upper water-column stratification (S) relative to those of deep mixing (DM), and blue shading in the calendar bars shows the typical timing of local rain seasons. (For interpretation of the references to color in this figure legend, the reader is referred to the Web version of this article.)

(e.g., 80 m: range 86−1495; mean = 740). Only ca. 9% of the SPM samples with detectable crenarchaeol had values of GDGT-0/crenarchaeol between 0 and 2, while 53% had values > 15 (Fig. 2B; Table S1). Average f[CREN'] and TEX$_{86}$ values are 0.05 and 0.28, respectively (Fig. S2C-D), but as cren' concentrations in the SPM were often too low for quantification (below detection limit in 43% of the samples), these values represent a limited dataset.

3.3. IPL isoGDGTs in SPM

Only IPLs with an GDGT-0 core were detected in the SPM of Lake Chala, but these were present at all analyzed depths (20, 30, 45 and 90 m) at the three selected dates (December 2013, April 2014 and September 2014; n = 12; Fig. 4). The absence of crenarchaeol and the other IPL isoGDGT is not surprising, because, as reported above, the CL + IPL concentrations (including those of acid-hydrolyzed IPL-derived GDGTs) of these GDGTs were generally low in the SPM. IPL GDGT-0 with a monohexose (MH) head-group was detected in 11 of the 12 samples, and is the dominant IPL in most of them. Also two isomers of dihexose (DH-) GDGT-0 with distinct retention times (here referred to as DH(1)- and DH(2)-) were detected, in 5 and 7 SPM samples, respectively The existence of distinct DH-GDGT-0 isomers may relate to an alternative configuration of one hexose moiety at each end of the lipid, or to a singular dihexose attached to one end (Besseling et al., 2018). In addition, phosphatidylglycerol (PG-), monohexose-phosphatidylglycerol (MH-PG-), and dihexose-phosphatidylglycerol (DH-PG-) GDGT-0 were detected in respectively 5, 3 and 2 samples. In December 2013, when the oxycline was at a shallow depth of ~15 m and therefore all analyzed depth intervals were situated in the anoxic zone, CL, MH- and DH(1)- GDGT-0 were most abundant at 20 and

30 m, and slightly less abundant in deeper water (Fig. 4A). Moreover, in December 2013 the two DH-GDGT-0 isomers clearly have a different distribution, with DH(1)- being relatively abundant at 20 and 30 m and lacking at 90 m, whereas DH(2)- is only present at 45 and 90 m. In April and September 2014, when the oxycline had deepened to ~25 and ~43 m, respectively, IPL amounts are clearly lowest in the oxygenated upper water column, and the abundance of both DH(2)- and MH-GDGT-0 increases with depth (Fig. 4B and C). IPLs with an additional phosphatidylglycerol (PG) head group, i.e. MH-PG and DH-PG-GDGT-0, were recovered almost exclusively at 90 m and only in April and September 2014 when the oxycline was more depressed. Also, the relative proportions of IPL GDGT-0 with the five different head groups recovered at 90 m are highly comparable between these two months.

3.4. Abundance and composition of archaea in SPM

The archaeal abundance estimated as the number of archaeal 16S rRNA gene copies L^{-1} (Table S5) displayed maximum values up to 10^5 archaeal cells L^{-1} (Fig. 5A). The anoxic water column, and particularly the lowermost water layer at 60−90 m depth, contained more archaeal cells than upper oxygenated waters (Fig. 5A). Archaeal 16S rRNA gene reads from anoxic water were mostly classified as Euryarchaeota (classes Methanomicrobia, Methanobacteria and Thermoplasmata), Bathyarchaea (Group C3 of the MCG) and Woesearchaea (DHVEG-6 Group). Thaumarchaeotal 16S rRNA gene copies were only represented by Group I.1b and not by Group I.1a, and were highest in the oxygenated part of the water column (Fig. 5B). In contrast, those of Bathyarchaea (Fig. 5D) and Euryarchaea (Fig. 5E) were highest in the anoxic zone. Although the latter reach peak values substantially higher than those of the
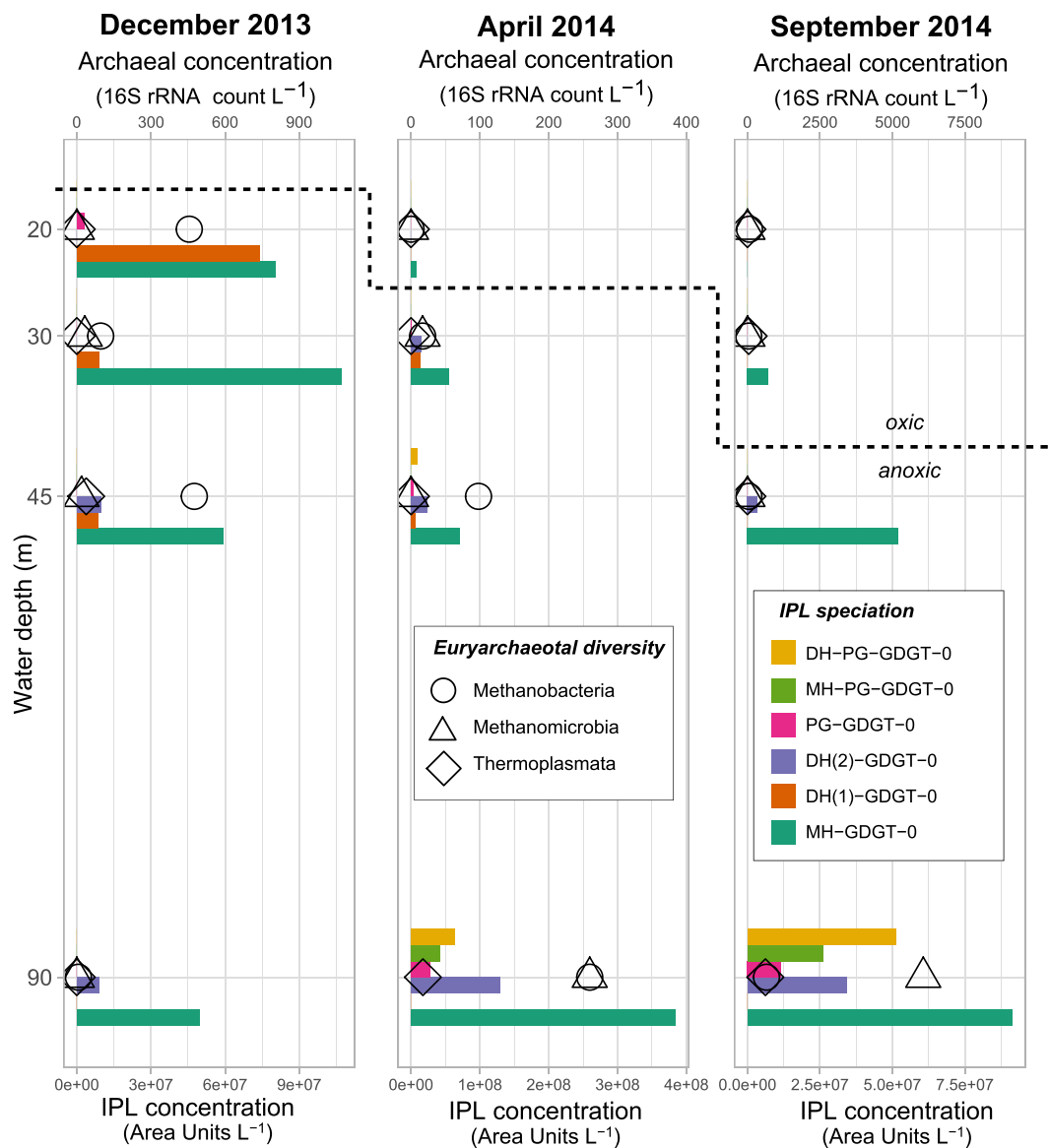
Fig. 4. Concentrations of IPL GDGT-0 with various head groups (colored bars; in Area Units L^{-1}) and concentrations of archaeal 16S rRNA (open symbols; in gene copies L^{-1}) for select groups of Euryarchaea in Lake Chala SPM collected in December 2013 (A), April 2014 (B) and September 2014 (C). The varying position of the oxic-anoxic boundary (oxycline) is indicated with the horizontal dashed line.

Thaumarchaeota, above the oxycline Thaumarchaeota often represented 60–100% of the total archaeal 16S rRNA gene reads (Fig. 5C).

3.5. CL + IPL isoGDGTs in settling particles

All CL + IPL isoGDGTs analyzed were detected in the settling particles captured at 35 m depth, both in periods with shallow oxycline (September to March) and periods with deep oxycline (August to November; Fig. 6 and Table S3). In contrast to the distribution of CL + IPL isoGDGTs in SPM, crenarchaeol was the dominant isoGDGT in about half of the samples (48 out of 98), and displayed monthly fluxes ranging over three orders of magnitude (from 0.002 to 9.2 μg m^{-2} day^{-1}; Fig. 6E). GDGT-0 dominated in the other half (50 out of 98), with a flux varying from 0.009 to 5.3 μg m^{-2} day^{-1} (Fig. 6D) and occasionally amounting to 99% of the summed isoGDGT flux. Fluxes of GDGT-1, -2, -3 and cren' were minor in comparison, with fractional abundances typically <0.1.

Temporal variation in the fluxes of all isoGDGTs except GDGT-0 are highly similar throughout the study period and strongly correlated (R^2 between 0.67 and 0.97, $p < 0.001$). The flux of GDGT-0 is weakly correlated to that of crenarchaeol, and only between September 2010 and January 2015 (R^2 = 0.11, $p = 0.02$, $n = 53$); the correlation disappears when data from November 2006 to August 2010 (Sinninghe Damsté et al., 2009; Buckles et al., 2014, 2016) are included (R^2 = 0.01, $p = 0.27$, $n = 98$). Short-lived peaks in crenarchaeol flux occur fairly regularly through the eight-year study period, but these are sometimes separated by periods of low crenarchaeol flux lasting several years (e.g. 2008–2009 and 2013–2014; Fig. 6E). The GDGT-0/crenarchaeol ratio ranges widely from 0.06 to 274 (on average 27 ± 52; Fig. 6G), but its maximum value is still five times smaller than that found in SPM. The most elevated GDGT-0/crenarchaeol values occur from July to November 2008, August to November 2009, in September 2010, and continuously from September 2013 until September 2014 (Fig. 6G). These high GDGT-0/crenarchaeol values are a result of both low
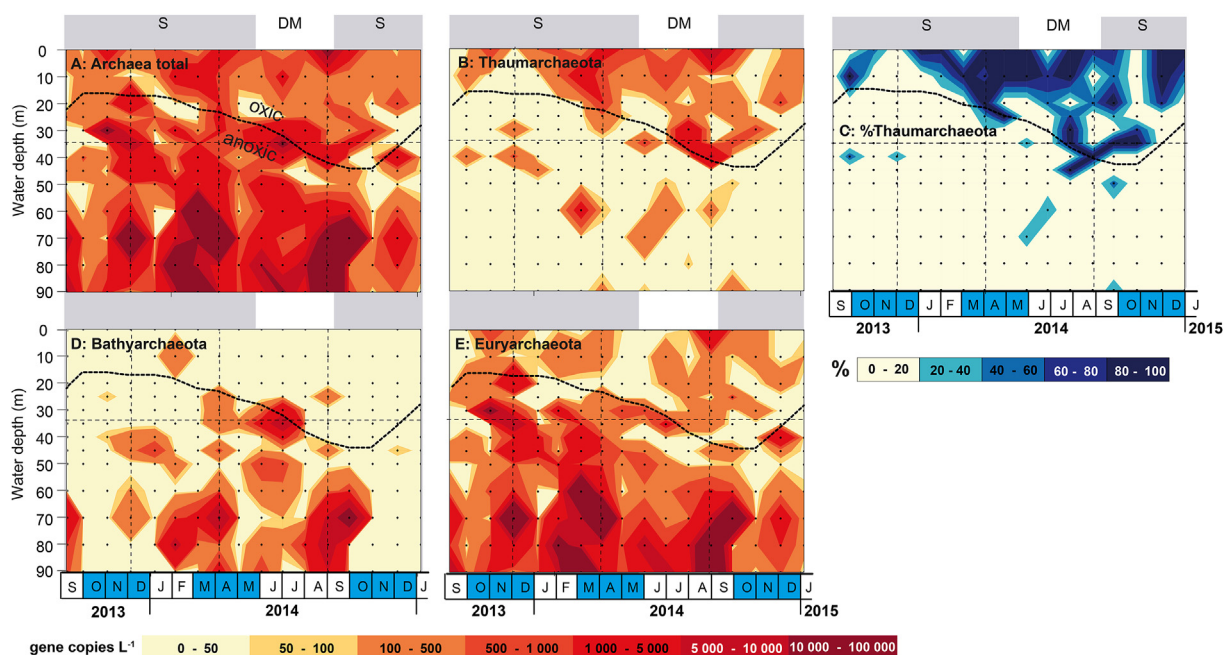
Fig. 5. Interpolated concentrations of archaeal 16S rRNA (in gene copies L^{-1}) in SPM from Lake Chala collected at approximately monthly intervals between September 2013 and January 2015. Concentrations of the sum of all archaea (A), Thaumarchaeota, here exclusively Thaumarchaeota Group I.1b (B), the relative abundance (%) of archaeal gene copies which belong to Thaumarchaeota (C), Bathyarchaeota, predominantly comprised of Bathyarchaeota Group C3 (D), and Euryarchaeota, dominated by methanogenic Methanomicrobia and Methanobacteria (E). The varying position of the oxic-anoxic boundary (oxycline, or depth to anoxia; van Bree et al., 2020), the static position of the sediment trap (thin horizontal dashed line at 35 m depth) and the SPM sampling grid (black dots) are also indicated. Vertical dashed lines indicate the three months for which IPL GDGTs were also analyzed. The grey background shading shows the seasonal periods of upper water-column stratification (S) relative to those of deep mixing (DM), and blue shading in the calendar bars shows the typical timing of local rain seasons. (For interpretation of the references to color in this figure legend, the reader is referred to the Web version of this article.)

crenarchaeol and high GDGT-0 fluxes. The f[CREN'] ranged between 0.01 and 0.33 (average 0.07 ± 0.06, $n = 92$) and is highest when both the GDGT-0/crenarchaeol ratio and BIT-index values are high (Fig. 6H). TEX$_{86}$ values range from 0.48 to 0.86 (0.69 ± 0.08 on average, $n = 94$; Fig. S2D). The BIT index ranges from 0.09 to 1.0 and is on average 0.73 ± 0.28 (Fig S2A). It is low (<0.50) during periods of high crenarchaeol fluxes, and consistently high (>0.90) from August 2008 to November 2009 and from September 2013 to January 2015, when the crenarchaeol flux is virtually zero (Fig. 6E and F). Prolonged periods of high BIT values also coincide with periods with high GDGT-0/crenarchaeol ratios and high f[CREN'] values (Fig. 6).

4. Discussion

4.1. Spatiotemporal distribution of CL and IPL isoGDGTs in the water column of Lake Chala

Overall, CL + IPL isoGDGT concentrations were substantially higher in the anoxic lower water column of Lake Chala (zones 3−6) than in the oxygenated upper water column (zones 1−2; Fig. 3A). IsoGDGTs were particularly abundant below 45−50 m depth, typically the greatest depth of seasonal mixing (Buckles et al., 2014). This pattern is especially strong in GDGT-0, which reaches relatively high concentrations in the ~30-20 m depth range when the oxycline was at a shallow position (Fig. 3C). Strikingly, within the unmixing lower water column, where abiotic conditions are stable throughout the year (i.e. 60-90 m, zones 4−6), the concentrations of CL + IPL GDGT-0 varied over time, and were somewhat higher during periods of stratification compared to the principal mixing season (Fig. 3C). This variability likely relates to seasonal variations in the amount of decaying algae sinking into these water layers from the upper water column. The high CL + IPL GDGT-

0 concentrations are also reflected in the exceedingly high values of the GDGT-0/crenarchaeol ratio in this part of the water column throughout our monitoring period (up to 1500 at 80 m in November 2014; Table S2), substantially higher than in earlier studies of the water column (maximally 38 at 90 m in September 2006 (Sinninghe Damsté et al., 2009) and 32 at 80 m in January 2010 (Buckles et al., 2013), although this difference may partly relate to the acid-hydrolysis step in our work-up procedure (see section 2.3.2) which brings IPL GDGT-0 into our analytical window. In any event, the oxycline depth clearly has an important influence on the production of GDGT-0 as reflected in the IPL concentrations, which are present in much higher amounts in the anoxic zone of the water column compared to the oxygenated upper layer (Fig. 4). Moreover, individual IPLs of GDGT-0 displayed different spatio-temporal distributions below the oxycline. For example, the two DH-isoGDGT isomers had different depth distributions from one another, and the IPLs of PG-, MH-PG and DH-PG-GDGT-0 were almost entirely restricted to the lowermost water column (90 m depth) in April 2014 and September 2014. To date, the occurrence of IPL isoGDGTs with PG-containing head groups had been rarely reported in natural settings. They have been identified in the marine environment (e.g. Schubotz et al., 2011; Yoshinaga et al., 2011; Rossel et al., 2011; Sollai et al., 2019), and also in the anoxic sediment of the White Oak River estuary (Meador et al., 2015), but to the best of our knowledge they have not previously been identified in lakes. Whereas temperature is relatively constant throughout the anoxic zone (between 22.3 °C at the bottom and typically ~23 °C at the top; Fig. 2A), the amount of dissolved solids increases significantly between ~55 and ~65 m depth (Barker et al., 2013; Wolff et al., 2014; expressed as electrical conductance (conductivity) in Fig. 2D), a steep pH gradient occurs between ~40 and 65−70 m depth (Buckles et al., 2014; Wolff et al., 2014, Fig. 2C), and the concentration of methane increases sharply between ~40 and
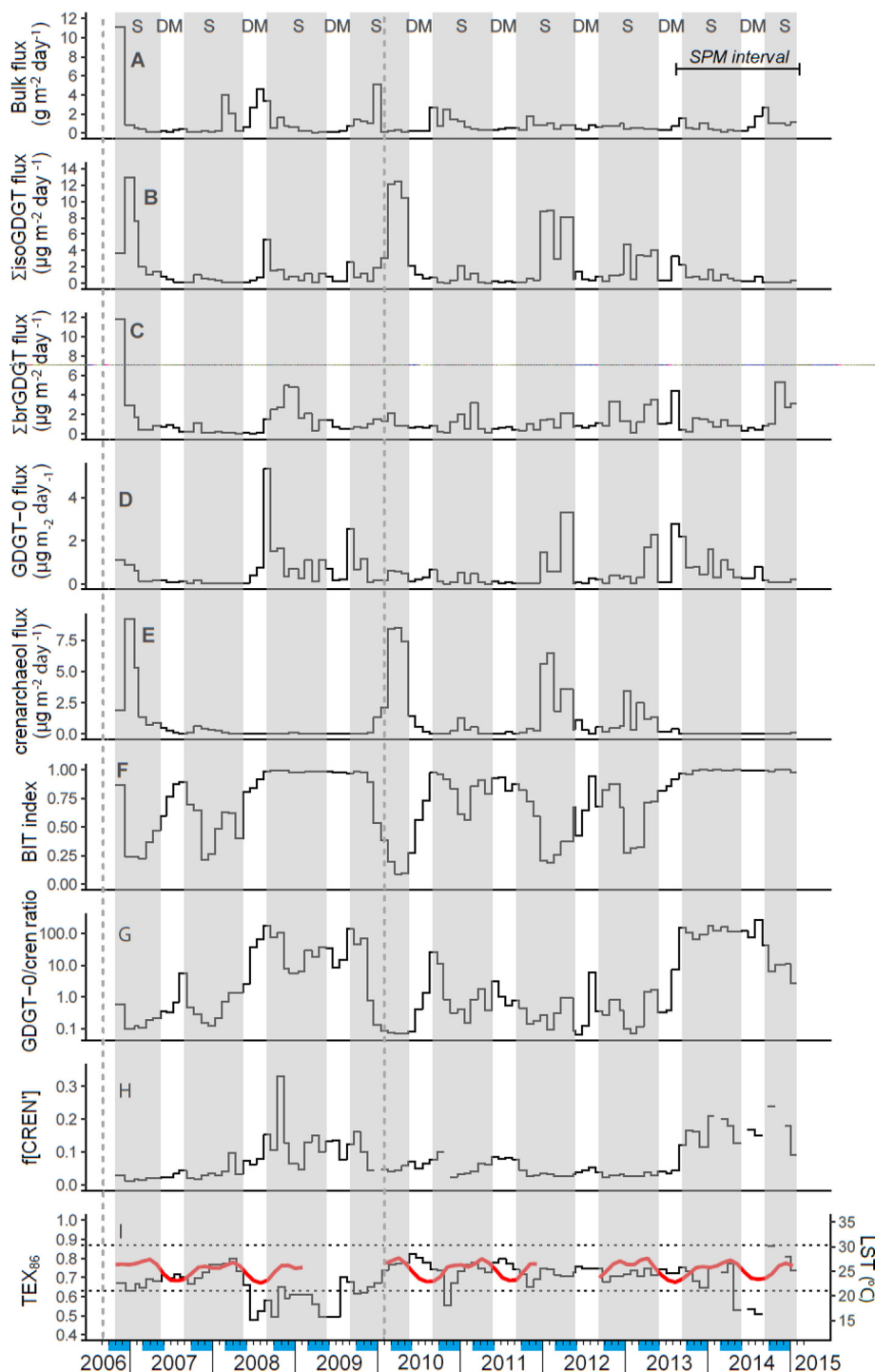
Fig. 6. Temporal variation in the daily flux ($\mu g\ m^{-2}\ day^{-1}$) of isoGDGTs in settling particles in Lake Chala, trapped at 35 m depth and collected at approximately monthly intervals between November 2006 and January 2015 ($n = 98$), and resulting temporal variation in derived GDGT proxies. Shown are the fluxes of bulk dry matter (A; in $mg\ m^{-2}\ day^{-1}$), all isoGDGTs (B), all brGDGTs (C), GDGT-0 (D) and crenarchaeol (E), and temporal variation in BIT index (F), GDGT-0/crenarchaeol ratio (G), f[CREN'] (H) and TEX_{86} (I). Also indicated are the TEX_{86}-derived lake surface temperatures (LSTs), calculated with the Tierney et al. (2010) calibration (right axis in panel I). Horizontal dashed lines in panel (I) mark the range of plausible TEX_{86} values for settling particles during this interval (0.63−0.87); see text. The thick red line in (I) represents the 'mixed layer' temperature (average of 2 and 10 m) time series measured by automatic temperature loggers (Buckles et al., 2014; van Bree et al., 2020). Samples/months in which the crenarchaeol isomer abundance is below detection (and thus f[CREN'] = 0), and samples/months lacking the minor isoGDGTs (i.e. TEX_{86} = NA) are represented as gaps in panels (H) and (I), respectively. Data from November 2006 to August 2010 are from Sinninghe Damsté et al. (2009) and Buckles et al. (2013), those from September 2010 onward are new to this study. The background shading shows the seasonal periods of upper water-column stratification (S) and deep mixing (DM). Blue shading in the calendar bars shows the typical timing of local rain seasons. For reference, also indicated are the 17-month period of SPM monitoring in this study, and the collection date of SPM analyzed by Sinninghe Damsté et al. (2009; September 2006) and Buckles et al. (2013; February 2010). (For interpretation of the references to color in this figure legend, the reader is referred to the Web version of this article.)

~60 m (Fig. 2E). Therefore, observed differences in the variety and distribution of IPLs of GDGT-0 within the anoxic zone may be due to the influence of strong chemical and redox gradients in the lower water column of Lake Chala (Wolff et al., 2014) on the niches available to GDGT-0 producers.

The concentration of crenarchaeol in the water column of Lake Chala was generally low during our 17-month monitoring period (0.09 ng L^{-1} on average), but it was detected in most SPM samples from water above the oxic-anoxic boundary, albeit always in low concentrations (<0.3 ng L^{-1}). The crenarchaeol concentrations found in this study are of the same order of magnitude as those recorded during the deep mixing season in September 2006, when its concentration increased with depth from 0.06 to 0.2 ng L^{-1} within the upper oxygenated water, and subsequently from 0.4 to 1.8 ng L^{-1} in anoxic waters from below the oxycline to 80 m depth (Sinninghe Damsté et al., 2009). In strong contrast, under stratified conditions in February 2010 the crenarchaeol profile showed a distinct maximum (3.5 ng L^{-1}) just above the oxycline at 39 m that was mirrored by a clear peak in IPL-derived crenarchaeol (1.0 ng L^{-1}; Buckles et al., 2013). In our data (reflecting combined CL and IPL crenarchaeol, see section 2.3.2), such peaks are of lower magnitude and restricted to narrow depth ranges within the lower water column that vary over time, but do not show a clear contrast between stratified and mixing periods as could be expected based on the two previous studies. The apparently narrow depth niche of crenarchaeol production at any one time between September 2013 and January 2015 suggests that crenarchaeol production was low throughout this period, further supported by our finding that IPLs with a crenarchaeol core lipid could not be detected, implying no substantial "live" production of crenarchaeol. Limited crenarchaeol production is also suggested by the very low crenarchaeol concentration in settling particles during this period (Fig. 6E; see section 4.4).

4.2. Spatiotemporal distribution of archaeal groups in the water column of Lake Chala

In line with Buckles et al. (2013) and the isoGDGT data discussed above, the composition of archaeal communities in Lake Chala differed substantially between the oxic and anoxic parts of the water column, and also displayed substantial temporal variation (Fig. 5). Overall, however, archaeal gene abundances were very low with maximum abundances on the order of 10^4 cells L^{-1}, i.e. close to the limit of detection. Unexpectedly, this is much lower than in February 2010 (Buckles et al., 2013), where total archaeal 16S rRNA gene abundances ranged from 4 × 10^3 to 2 × 10^7 copies L^{-1} (using the Parch519F-Arc915R primer pair; maximum at 24 m depth) and from 7 × 10^4 to 8 × 10^7 copies L^{-1} (using the Arc344F-Arc915R primer pair; maximum between 69 and 82 m). These major differences suggest that the abundance of archaea in Lake Chala is highly variable between years. Together with our data on isoGDGT concentrations in SPM and settling particles, it appears that the 17-month SPM-monitoring period of this study is characterized by an exceptionally low amount of archaea and, consequently, archaeal biomarkers.

Notwithstanding these low archaeal abundances, several interesting patterns occur in the composition and distribution of archaea in the water column of Lake Chala. Archaea of Group I.1b Thaumarchaeota were mainly restricted to the upper water column, in agreement with the finding of Buckles et al. (2013) for February 2010. The lower depth limit of Thaumarchaeota during the SPM-monitoring period follows the oxycline (Fig. 5B), indicating a close association of these ammonia-oxidizing archaea with the abiotic conditions in this specific aquatic habitat. Notably, their continuous presence between March and October 2014, and peak

depth-integrated concentrations during the principal dry season from July to September 2014, appear to argue that deep mixing and subsequent nutrient recycling is a greater driver of Thaumarchaeota production than rain-induced runoff from catchment soils as suggested earlier (Buckles et al., 2016). Members of Thaumarchaeota Group I.1a were not detected in this study, although they formed a substantial part of the thaumarchaeotal community in February 2010 when they bloomed at ~40 m depth (Buckles et al., 2013) and in September 2006 in waters above the oxycline (Sinninghe Damsté et al., 2009).

Group C3 archaea, a subgroup of MCG Bathyarchaeota (MCG-15; Kubo et al., 2012; Lavergne et al., 2018; Zhou et al., 2018) are mainly restricted to anoxic waters in Lake Chala (Fig. 5D). During the 17-month SPM monitoring period they occurred most prominently in the lowermost zone of the water column (60–90 m), similar to their depth distribution in February 2010 (Buckles et al., 2013). Although the elevated conductivity (i.e., the amount of dissolved solids, and hence water density, cf. above) of this depth zone (Fig. 2) prevents seasonal mixing, and therefore abiotic conditions in this permanently stratified part of the water column can be expected to remain fairly constant through time, concentrations of these Bathyarchaeota display large temporal variation (Fig. 5D). Bathyarchaeota are a highly diverse group of archaea (Kubo et al., 2012), but because they have not been cultured, their metabolism is at present unclear. It has been suggested (e.g., Zhou et al., 2018) that they are metabolic generalists, specialized in degrading recalcitrant organic matter under anoxic conditions. It is therefore possible that seasonal variation in their occurrence may reflect the variable input of complex organic matter settling into this depth zone from higher up in the water column.

Methanobacteria and Methanomicrobia were relatively dominant in the anoxic water column of Lake Chala (Fig. 5E). Although they also occurred in comparatively low absolute abundances throughout the 17-month SPM monitoring period, their concentrations peaked in the permanently stratified lowermost water column between 60 and 90 m depth, where also the highest methane concentrations occur (Fig. 2). It is therefore feasible that these archaeal taxa are involved in methanogenesis in Lake Chala, together with Methanosarcinales, the only methanogens detected in February 2010 (Buckles et al., 2013) but not detected in this study.

Taking into account the generally very low abundances of archaeal 16S rRNA gene reads, the composition of the archaeal community in Lake Chala and the depth distribution of the various groups suggests that i) Thaumarchaeota I.1b mainly occur in oxygenated waters, ii) anaerobic heterotrophs of (Group C3) MCG Bathyarchaeota mainly occur in the lowermost water column, and iii) specific euryarchaeotal taxa occurring at these depths may be involved in methanogenesis.

4.3. Archaeal sources of Lake Chala isoGDGTs

To determine the source(s) of isoGDGTs in Lake Chala, isoGDGT concentrations were correlated to the estimated abundance of microbial groups inferred from 16S rRNA gene amplicon sequencing using the same methods previously applied to the brGDGTs (van Bree et al., 2020). Unfortunately, due to the exceptionally low abundances of archaea in the SPM during the 17-month study period, the few resulting significant correlations appeared to be driven by the absence or presence of archaeal genes rather than their range of abundance, and hence considered unreliable. Therefore, we determined the possible producers and environmental significance of isoGDGTs via qualitative comparison of the spatial and temporal patterns of isoGDGTs and archaeal gene copies in the SPM.

Firstly, considering the relationship between different isoGDGTs themselves, the similar temporal variation in the fluxes of all isoGDGTs, excluding GDGT-0, in settling particles captured at 35 m depth (Table S3; $R^2 = 0.67-0.97$, $p < 0.001$; $n = 98$) suggests that they are produced by the same group of microbes. The flux of GDGT-0 is not correlated to any of these ($R^2 < 0.02$), strongly indicating that it may predominantly be produced by (a) different group(s) of archaea. This contrast is also evident in the SPM: although isoGDGT concentrations are generally low, GDGT-0 has a clearly different distribution over time and with depth than other isoGDGTs (Fig. 3). Overall, the spatiotemporal distribution of GDGT-0 is most similar to that of the Bathyarchaeota (dominated by Group C3) and the Euryarchaea (dominated by Methanomicrobia and Methanobacteria), of which the highest numbers of 16S rRNA gene copies are all found in the lowermost part of the water column (Figs. 3C and Fig. 5D−E). This agrees well with previous findings, as GDGT-0 is the major GDGT in methanogenic archaea (see Schouten et al., 2013) and has previously been linked to Bathyarchaeota Group C3 in Lake Chala (Sinninghe Damsté et al., 2009; Buckles et al., 2013). Moreover, even qualitative comparison between variation in the concentrations of different IPL GDGT-0 forms and the numbers of archaeal gene copies in SPM profiles from the three selected time windows provides some indication which archaea may produce these lipids (Fig. 4). As was the case for the CL + IPL isoGDGTs, there appears to be some correspondence between IPL isoGDGTs and the 16S rRNA gene sequences of Euryarchaeota (Fig. 4). Specifically, in the two samples (i.e., depth/month combinations) with elevated amounts of PG-, DH-PG- and MH-PG-GDGT-0, gene counts of select Euryarchaeota (Methanomicrobia, Methanobacteria and/or Thermoplasmata) are also high compared to other depth intervals within the respective profiles. Previous studies have shown that methanotrophic and methanogenic archaea produce GDGTs with different head groups, with mixed hexose and phosphate-based IPLs (e.g. PG-, DH-PG- and MH-PG-GDGT) being abundant in methanogenic archaea (Koga et al., 1993; Strapoć et al., 2008; Schubotz et al., 2011), whereas DH-GDGT was the dominant IPL of methanotrophic archaea (Rossel et al., 2008, 2011). Thus, the spatiotemporal differences between hexose and mixed hexose/phosphate-based IPL GDGTs, may indicate different metabolic processes occurring in the water column of the lake.

Thaumarchaeota are the only known producers of crenarchaeol so far (Schouten et al., 2013 and references therein; Bale et al., 2019b), and the general occurrence of thaumarchaeotal gene copies in the oxygenated upper water column (Fig. 5B and C) is in good agreement with the spatiotemporal distribution of crenarchaeol in SPM (Fig. 3D). Previously, crenarchaeol in the upper water column of Lake Chala has been attributed to production by Thaumarchaeota of both Group 1.1a and 1.1b (Sinninghe Damsté et al., 2009; Buckles et al., 2013). In this study, Group I.1a Thaumarchaeota were not detected, suggesting that Group I.1b was primarily responsible for crenarchaeol production in 2013−2014. Short-lived local peaks of crenarchaeol in the anoxic zone, for example in the well-resolved depth profiles from November 2013 and August 2014 (Fig. 3C), do not fully match local maxima in 16S rRNA gene copies of Group I.1b Thaumarchaeota (Fig. 5B), as was also the case in the SPM profile from February 2010 (Buckles et al., 2013). This mismatch, and the somewhat unexpectedly high abundance of crenarchaeol in the lowermost water column (60−80 m) can likely be explained by the different stage of degradation that they represent: whereas the spatiotemporal distribution of Group I.1b Thaumarchaeota gene copies more closely represents the ecological niche of the living archaea, the highly stable CL isoGDGTs remain intact while sinking through the water column into the permanently stratified deepest water where

optimal conditions for preservation promote their accumulation over time. A similar observation has been made for thaumarchaeotal DNA and isoGDGTs in the stratified Black Sea (Coolen et al., 2007).

The remarkably low number of archaeal 16S rRNA gene copies and low concentrations of crenarchaeol and total isoGDGTs in SPM during the 17-month study period (the latter also in settling particles) indicate that no thaumarchaeotal, or archaeal bloom in general, occurred in Lake Chala between September 2013 and January 2015. This intermittent (near-) absence of Thaumarchaeota was previously noted by Buckles et al. (2014, 2016), on the basis of low or non-existent crenarchaeol flux in settling particles during large parts of 2008 and 2009 (Fig. 6E).

Our detailed analysis of the Lake Chala water column shows that Thaumarchaeota are mainly restricted to the upper oxygenated zone such that low concentrations (or absence) of crenarchaeol coincide with a persistently shallow (~15 m depth) oxycline during episodes of strong stratification (Fig. 3D). Thus, due to their reliance on oxygen to perform ammonia oxidation, the niche available for Thaumarchaeota growth becomes more restricted during episodes of strong and typically relatively shallow upper-water-column stratification. Additionally, it has been shown that ammonia-oxidizing archaea (AOA), i.e. Thaumarchaeota, exhibit greater photoinhibition than ammonia-oxidizing bacteria (AOB; Merbt et al., 2012). Photoinhibition may be a pertinent environmental driver in the nutrient-starved Lake Chala, where excepting the diatom-bloom months of July−September (Wolff et al., 2011) the water transparency measured as Secchi-disk depth (typically 5−8 m during stratified periods; van Bree et al., 2018) equals or exceeds that of the most transparent among 60 crater lakes in western Uganda (Nankabirwa et al., 2019). Therefore, during episodes of strong stratification when Thaumarchaeota are restricted to the uppermost water layer where light is the most intense, they may be outcompeted by less photo-sensitive AOB. Together, these two factors (compression of the oxygenated zone and competition with less photo-sensitive AOB) likely suppress blooms of Thaumarchaeota.

4.4. Long-term isoGDGT trends in settling particles: implications for application of the BIT index and TEX_{86}

The unique eight-year sediment-trap record of Lake Chala shows large variation in isoGDGT composition and fluxes over time that cannot easily be related to the seasonal alternation of strong water-column stratification and deep mixing (Fig. 6), even though this was seen to exert primary control on the distribution of archaeal species and GDGTs in the 17-month time series of SPM. This prompts the question of what these longer-term trends in the GDGT ratios of settling particles actually represent.

Strikingly, over the 98-month period of settling-particle data crenarchaeol flux appears to drive variation in both the BIT index and the GDGT-0/crenarchaeol ratio (Fig. 6E−G, 7), as was noted before based on concentration profiles of brGDGTs and isoGDGTs in SPM (Sinninghe Damsté et al., 2012a; Buckles et al., 2014, 2016). Our 17-month SPM dataset in combination with two single profiles from earlier years (Sinninghe Damsté et al., 2009; Buckles et al., 2013) indicated that Thaumarchaeota live in the upper oxygenated layer of the water column, whereas GDGT-0 is predominantly produced below the oxycline. As the sediment trap was suspended at 35 m depth, a high relative abundance of GDGT-0 to crenarchaeol in the settling particles implies that the oxycline must have been located above this level. Similar to GDGT-0, also the brGDGTs in Lake Chala were found to be produced mainly in the anoxic part of the water column and most abundantly so during periods of strong stratification (van Bree et al., 2020). Thus, periods with a
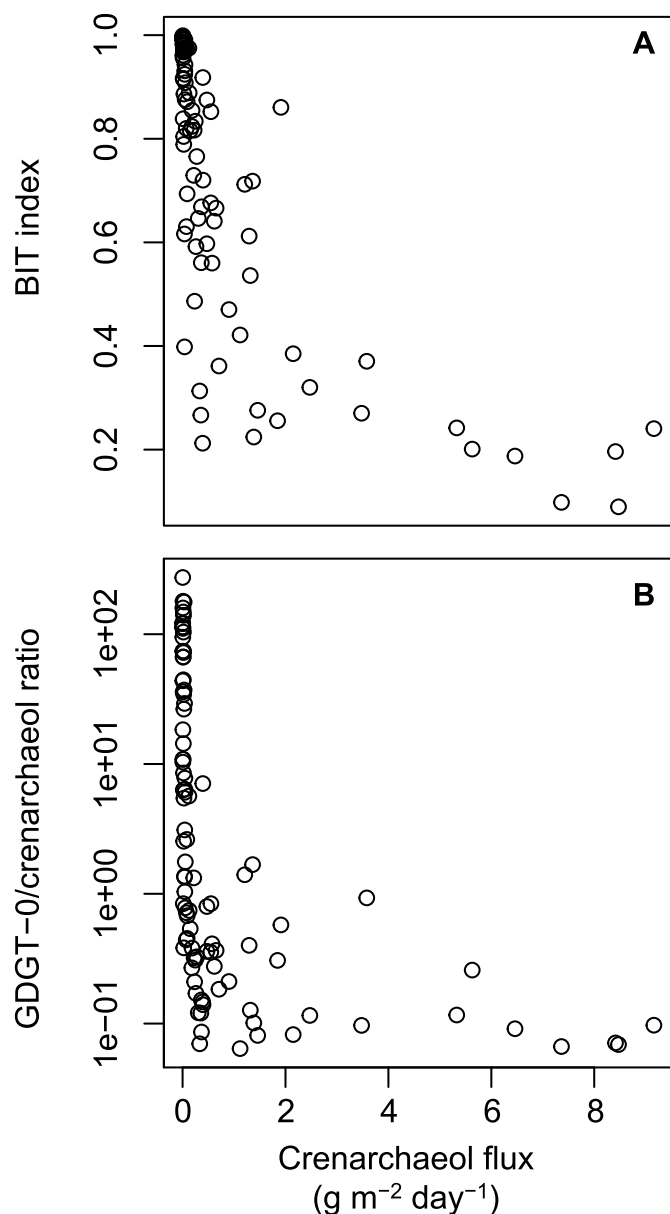
Fig. 7. Scatter plots of BIT index (A) and GDGT-0/crenarchaeol ratio (B) of settling particles in Lake Chala versus the monthly flux of crenarchaeol (in $\mu g\ m^{-2}\ day^{-1}$) measured over the eight-year sampling period ($n = 98$).

predominantly shallow oxycline (<35 m) are likely characterized by both high GDGT-0/crenarchaeol ratio and high BIT index in the settling particles. The two long periods of continuously high GDGT-0/crenarchaeol ratio and BIT index values in the settling particles, from June 2008 to November 2009, and from August 2013 to January 2015 (Fig. 6F and G) are thus indicative of sustained periods of exceptionally shallow oxycline conditions. Indeed, during the concurrent interval of SPM collection (September 2013−January 2015) the oxycline was most often located above 35 m (Fig. 3).

This result prompts re-evaluation of the mechanism by which longer-term BIT-index variation in the sediment record of Lake Chala may be related to climate variability. Rather than linking high BIT index values to an increased input of soil-derived brGDGTs in precipitation-induced runoff (cf. Weijers et al., 2007; Blaga et al., 2009; Verschuren et al., 2009), nutrient-induced Thaumarchaeota enhancement (Sinninghe Damsté et al., 2012a) or thaumarchaeotal

bloom suppression (Buckles et al., 2016), we here explain variation in the BIT index by the influence of stratification, and thus oxycline position, on the community composition of archaea in Lake Chala. At the inter-annual time scale, the seasonal duration of water-column stratification in Lake Chala is influenced by the strength of the monsoon (Wolff et al., 2011). Higher monsoonal wind speeds associated with dry conditions generate more extensive mixing of the upper water column, cutting stratification short. Conversely, lower wind speeds associated with rainy periods result in weaker mixing and allow an increasingly strong temperature stratification of the upper water column, further limiting oxygen renewal at depths below the daily mixed uppermost water layer. This ineffective oxygen renewal combined with ongoing decomposition of organic matter sinking out of the photic zone results in a progressive shallowing of the oxycline (cf. Fig. 2: zone 3 expands at the expense of zone 2), in turn expanding the anoxic habitat of GDGT-0 and brGDGT producers relative to that of the crenarchaeol producers. Hence, the shallower the oxycline, the further restricted becomes the Thaumarchaeota habitat.

During prolonged periods of high GDGT-0/crenarchaeol ratio and BIT index values and, hence, inferred strongly stratified conditions, f[CREN'] in settling particles tends to increase gradually over time (Fig. 6H). f[CREN'] reaches values up to 0.24 during the two such periods in 2008−2009 and 2013−2014, substantially higher than those attained in the 25-kyr sediment record of Lake Chala (Fig. 8D; typically ~0.02, with intermittent peaks up to 0.15; Sinninghe Damsté et al., 2012a). Several studies have shown that Group I.1a Thaumarchaeota typically produce 0−3% of the crenarchaeol isomer (relative to all isoGDGTs), whereas Group I.1b Thaumarchaeota produce 14−29% (e.g., Pitcher et al., 2010, 2011; Kim et al., 2012; Sinninghe Damsté et al., 2012b; Elling et al., 2017; Bale et al., 2019b), and therefore periods of elevated f[CREN'] likely relate to dominance of Group I.1b Thaumarchaeota. Indeed, elevated values of f[CREN'] in settling particles during the SPM-monitoring period in 2013−2015 (on average 0.16) are consistent with absence of Group I.1a Thaumarchaeota gene copies in the SPM during this time interval. As Group I.1b Thaumarchaeota were thought to grow more abundantly in soils in contrast to the aquatically produced Group I.1a Thaumarchaeaota, Sinninghe Damsté et al. (2012a) interpreted periods of high f[CREN'] in the sediment record of Lake Chala as indicating increased input of soil-derived Thaumarchaeota. However, it is unlikely that high f[CREN'] values between September 2013 and January 2015 are due to a temporally elevated influx of soil-derived isoGDGTs, as there is generally little input of terrestrial organic matter (van Bree et al., 2018) and no evidence of a marked increase in anthropogenic disturbance within Chala crater around that time. Whereas only Group I.1b Thaumarchaeota gene copies were detected in SPM collected between September 2013 and January 2015, gene copies of both groups were detected in SPM obtained in September 2006 (Sinninghe Damsté et al., 2009) and February 2010 (Buckles et al., 2013). Notably, in the settling particles record these months also showed low f[CREN'] values (Fig. 6H). Importantly, in both of these earlier SPM profiles Group I.1a Thaumarchaeota occur abundantly only just above the oxycline (located at 43−47 m at that time), while Group I.1b Thaumarchaeota were relatively dominant in the uppermost water layers (Sinninghe Damsté et al., 2009; Buckles et al., 2013), as they were during our 17-month SPM monitoring period. It thus appears that the two groups occupy distinct depth zones in Lake Chala, and, consequently, in addition to oxycline depth controlling the general proliferation of Thaumarchaeota and therefore crenarchaeol abundance and dependent proxies (BIT index and GDGT-0/crenarchaeol ratio), it also impacts the proportion of Group I.1a versus I.1b Thaumarchaeota and thus f[CREN']. Based on our current data, Group I.1a Thaumarchaeota may be more
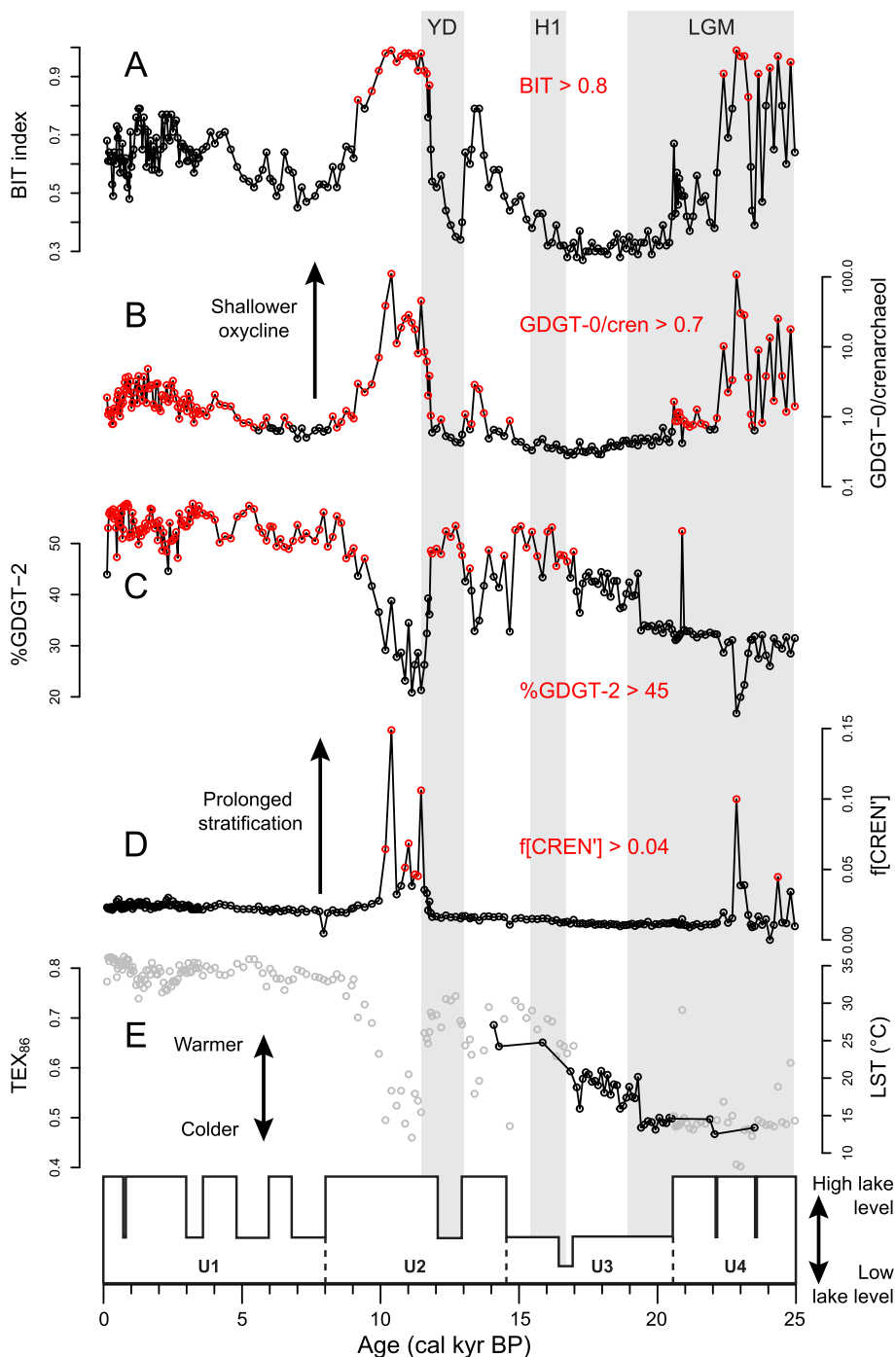
Fig. 8. Temporal variation in BIT index (A; from Verschuren et al., 2009); (B) GDGT-0/crenarchaeol ratio (B); %GDGT-2 (C), f[CREN'] (D) and TEX$_{86}$ (E; the latter all modified after Sinninghe Damsté et al., 2012a) in the 25-kyr sediment record of Lake Chala, compared with the succession of lake high- and low-stands based on seismic-reflection stratigraphy (F; from Moernaut et al., 2010). In panels A–D, GDGT proxy values outside the boundaries proposed for reliable TEX$_{86}$-based temperature reconstruction are indicated in red; see text. In panel E, reliable TEX$_{86}$ datapoints are plotted in black, while compromised values are plotted in light grey. The shaded areas represent the Last Glacial Maximum (LGM; 23–19 ka BP), Heinrich event H1 (16.8–15.4 ka BP) and the Younger Dryas period (YD: 13–11.5 ka BP). (For interpretation of the references to color in this figure legend, the reader is referred to the Web version of this article.)

sensitive to light and hence proliferate in Lake Chala only when oxygen is present at depths well below 35 or even 40 m. Due to sporadic occurrence of the crenarchaeol isomer and generally low archaeal gene counts in the Lake Chala SPM analyzed in this study, the exact biological link between high proportions of cren' to crenarchaeol and a shallow oxycline remains unresolved at this time. Nonetheless, the direct relationship between f[CREN'] and the

proportion of Group I.1b versus I.1a Thaumarchaeota suggests that it may be a valuable indicator of prolonged upper water-column stratification.

The distribution of isoGDGTs in settling particles collected between November 2006 and December 2007 translated into TEX$_{86}$ values that reflected mean-annual LST fairly well, although the ~5 °C seasonal variation in LST was not captured (Sinninghe Damsté

et al., 2009). Our eight-year sediment-trap record now indicates that periods with low crenarchaeol concentrations, high BIT index, high GDGT-0/crenarchaeol ratio and high f[CREN'] values (i.e., shallow oxycline conditions and relative suppression of thaumarchaeota) tend to generate TEX_{86} values that underestimate LST (Fig. 6I). This is likely because during episodes of reduced thaumarchaeotal abundance a greater proportion of GDGT-1, -2 and -3 are produced by Euryarchaeota and/or Crenarchaeota, which do not have the same temperature dependency of ring formation as Thaumarchaeota (Schouten et al., 2013). In particular, the fractional abundance of the crenarchaeol isomer, which is only known to be produced by Thaumarchaeota, will be diluted compared to GDGT-1, -2 and -3, generating a cold bias in TEX_{86}. Notably, Group I.1b Thaumarchaeota do not produce isoGDGTs with the same temperature relationship as seen in Group I.1a (e.g. Elling et al., 2017). Therefore, the TEX_{86} index may not reliably reflect LST when environmental conditions create a prolonged shallow oxycline and Group I.1a Thaumarchaeota fail to bloom.

On the upside, comparison of the TEX_{86} values generated by settling particles with the tell-tale indicators of inadequate isoGDGT production by Group I.1a Thaumarchaeota (BIT, GDGT-0/crenarchaeol, f[CREN']) helps define precise limits for filtering out biased TEX_{86} values in order to identify those time intervals when

the isoGDGTs in Lake Chala truly recorded LST (Fig. 9). Considering the 5.1 °C seasonal temperature range of the daily-mixed upper water layer in Lake Chala between November 2006 and January 2015 (22.5−27.6 °C; Fig. 6I; van Bree et al., 2020), and estimated calibration error of 2.1 °C for the TEX_{86}-based LST inference model (Tierney et al., 2010), we conservatively calculate plausible settling-particle TEX_{86} values to range between 0.63 and 0.87. The TEX_{86} values actually recorded during the eight-year study period never exceed this range, but 22 monthly samples fall below this range (Figs. 6I and 9). In months when TEX_{86} values fall below 0.63, the BIT index is always >0.8, f[CREN'] > 0.04, and GDGT-0/crenarchaeol >0.7 (Fig. 9A−C). Filtering of the settling-particle data based on these boundaries results in TEX_{86} values with quasi-normal distributions within the range considered realistic (Fig. 10). While these boundaries are based on the temporal distribution of isoGDGTs produced in the upper 35 m of the water column and therefore do not take into account the deep-water production, the BIT index and GDGT-0/crenarchaeol ratio increase with depth (Fig. 3C-D; van Bree et al., 2020), implying that these proxies may still be used to set a conservative upper limit for realistic TEX_{86} values in the sediment record. However, a much larger fraction of the data will be filtered out. As deep-water isoGDGT production is unlikely to change the f[CREN'] ratio, this proxy may be preferred as
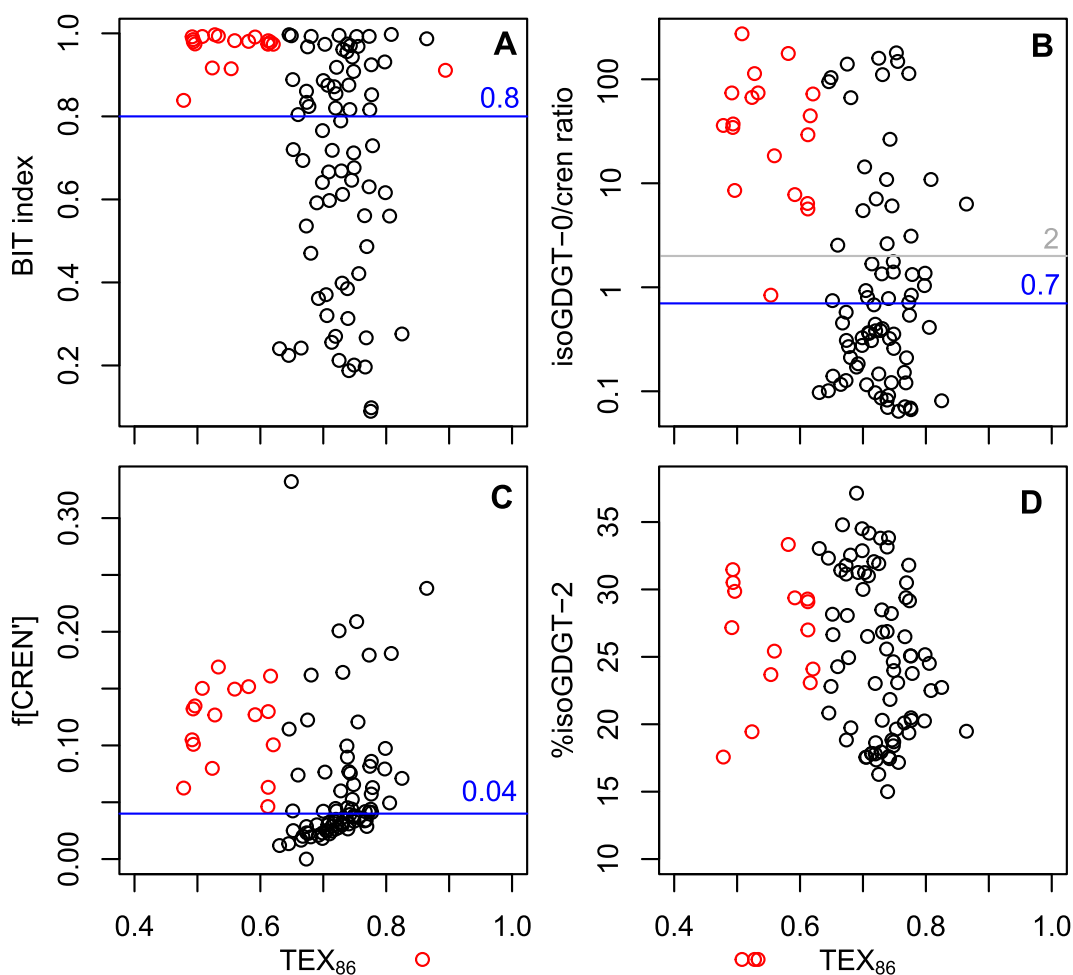
Fig. 9. Scatter plots of BIT index (A), GDGT-0/crenarchaeol (B), f[CREN'] (C) and %GDGT-2 (D) values versus the TEX_{86} values, obtained from those same samples of settling particles collected over an 98-month period in Lake Chala. Red open circles refer to samples with TEX_{86} values below the range of plausible TEX_{86} values for settling particles during this interval (0.63−0.87); see text. Blue lines indicate proposed boundaries (BIT >0.8, GDGT-0/crenarchaeol >0.7 and f[CREN'] > 0.04) above which TEX_{86}-based temperature estimate may be cold-biasedGDGT-0. The grey line in (B) indicates the previously used boundary for GDGT-0/crenarchaeol (>2; Sinninghe Damsté et al., 2012a). (For interpretation of the references to color in this figure legend, the reader is referred to the Web version of this article.)
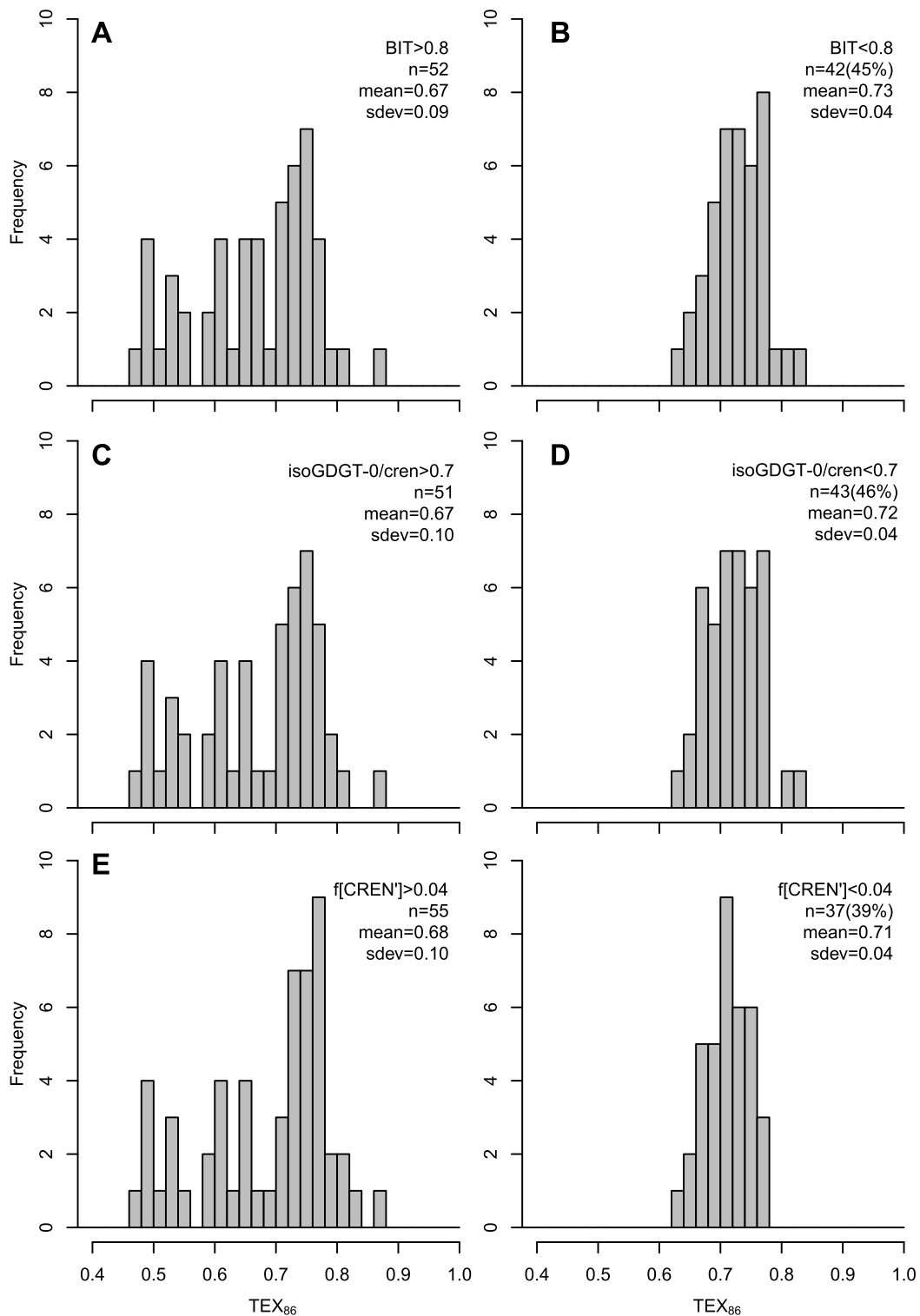
Fig. 10. Frequency distributions of data points with TEX$_{86}$ values above (left) and below (right) the boundaries indicated in Fig. 9 for BIT index (A–B), GDGT-0/crenarchaeol (C–D) and f[CREN'] (E–F).

filtering method in paleo-environmental applications. Of course, the boundaries proposed here are specific to Lake Chala; similar methods grounded in modern-system data should be used for testing the robustness of TEX$_{86}$ paleotemperature estimates in other lake systems.

4.5. Influence of oxygen on GDGT distributions in diverse lake systems

Similarly to Lake Chala, studies in both permanently stratified and seasonally mixed lakes have suggested that oxygen availability has a prominent role in determining the relative abundances and

spatial distributions of GDGTs as well as the predictive capacity of the TEX_{86} temperature proxy. In a shallow oligotrophic karst lake in the Catalan pre-Pyrenees (Spain), whereas TEX_{86} estimated temperatures from SPM in the upper water column were found to accurately predict measured values, SPM sampled from below the hypolimnion yielded TEX_{86}-LST estimates with a large error, indicating that isoGDGTs in the oxygen-depleted layer are likely produced by non-thaumarcheotal archaea and are not temperature dependent (Cao et al., 2020). Also, in a stratified lake in Norway, it was found that oxygen content greatly impacted the total concentration of isoGDGTs and that a high (low) isoGDGT-0/ crenarchaeol ratio corresponded to low (high) dissolved oxygen (DO) concentrations (Zhang et al., 2016). The relative abundance of isoGDGTs and their related indices in the surface sediments of a Chinese lake showed significant differences along the sampled DO gradient (Wu et al., 2021). In this lake, a high abundance of isoGDGT-0 was found in the low DO waters, which was matched by a higher abundance of Bathyarchaeota and methanogenic archaea (Wu et al., 2021). A study of CL and IPL isoGDGT distributions in the water column of Lake Malawi also speculated that two spatially distinct communities of Thaumarchaeota may exist in the lake, with the most abundant community residing in the upper oxygenation water column and a secondary community of deep-dwelling Thaumaechaota (possibly Group I.1b) living at the oxic/ anoxic boundary (Kumar et al., 2019). Comparing Lake Chala to other lake water column studies highlights the importance of oxygen content and, hence, lake stratification in the functioning of various isoGDGT based proxies, but large differences between these studies suggests that the arrangement of distinct zones occupied by GDGT producers in the water column is not universal amongst lakes, even when considering only permanently stratified lakes.

4.6. Implications for the sedimentary GDGT biomarker record

The large seasonal and inter-annual variability in isoGDGT content of settling particles in Lake Chala begs the question what their longer-term variations in the lake's sediment record actually represent. Overall, changes in the thickness of the oxygenated upper water layer appear to be key to understanding isoGDGT production in Lake Chala. As it exerts a major influence on isoGDGT signatures in the settling particles, it most probably also does on isoGDGT signatures incorporated in the lake's bottom sediments.

Importantly, the new insights generated by the present study, and in particular the finding that a shallow oxycline hampers Thaumarchaeota growth, justifies use of the BIT index as indirect rainfall proxy in this system over long time intervals, as was done by Verschuren et al. (2009), Sinninghe Damsté et al. (2012a) and Buckles et al. (2016). On longer time scales, periods with enhanced precipitation and reduced mean-annual wind speed will result in a greater frequency of shallow-oxycline conditions which shrink the Thaumarchaeota niche, meanwhile relatively expanding the anoxic zone of the water column where brGDGT product is greatest (van Bree et al., 2020). This reduces the proportion of crenarchaeol deposited in the sediments, thereby generating higher BIT values. In line with this, the sedimentary BIT record matches the first-order reconstruction of changes in lake depth over the past 25,000 years based on seismic stratigraphy (Fig. 8A and F; Verschuren et al., 2009; Moernaut et al., 2010). On the other hand, increased rainfall over long periods also increases lake depth itself, and thus the height of the anoxic zone and niche for brGDGT production. Thus, over long time periods, the two main controls on BIT variation, viz. Thaumarchaeota niche availability and total brGDGT production, can be envisioned as generally being both positively related to the local climatic moisture balance, reinforcing the BIT index as moisture-balance proxy. At the same time, the shallow-oxycline

mechanism of BIT-index variation may also explain discrepancies between the BIT record and other hydroclimate proxies from Lake Chala. Namely, the permanently stratified (meromictic) status of the lake is key to the functionality of the BIT index. If lake depth is reduced to the point that also the lowermost water layer is mixed and seasonally oxygenated, the BIT index may lose its sensitivity because stronger water-column mixing will not likely further increase the proportion of Thaumarchaeota to brGDGT producers. At the other extreme, when BIT-index values of 1 (no crenarchaeol present) are sustained over a long interval of time it cannot be ascertained whether the inferred high rainfall was stable throughout this interval or increased beyond a threshold which created a stratification and light regime that essentially kept Thaumarchaeota absent from the water column. Again, we reiterate that the response of the BIT index to local paleohydrology is likely lake-specific. For example, in Lake Qinghai on the Qinghai-Tibet Plateau, the BIT index was inversely related to lake level in both surface sediments and a sediment sequence of the last 12,000 years (Wang et al., 2012, 2016). Our mechanistic understanding of the BIT index outlined above should not be applied to the sediment records of other lake systems without thorough investigation into the occurrence of GDGTs in the modern lake system at those sites.

There is general agreement between the variability of GDGT indices in the 25-kyr sediment record and that observed in the settling-particles record, in that high BIT index, high GDGT-0/ crenarchaeol and high f[CREN'] are likewise correlated with each other and with lower-than-expected TEX_{86} temperature estimates (Fig. 8). This indicates that the processes influencing TEX_{86} estimates, as revealed by our studies of the modern lake system, also apply downcore and that the tell-tale indicators of shallow oxycline conditions identified here must be taken into account when filtering sediment horizons for TEX_{86}-based paleotemperature reconstruction. Sinninghe Damsté et al. (2012a) already noted that sediment horizons with high (>0.8) BIT values generally produced lower than expected LST estimates, but set no cut-off BIT value for exclusion of erroneous TEX_{86}-derived temperatures because evidence for in situ production of brGDGTs in the lake (Sinninghe Damsté et al., 2009) negated the use of this proxy as indicator of soil input (Sinninghe Damsté et al., 2012a). Our eight-year settling-particle record from Lake Chala linked to a time series of instrumental LST data reveals that BIT-index values > 0.8 do indeed correlate with unreliable temperature estimates, not because of soil-derived isoGDGT input but because of its relationship to Thaumarcheota niche extent. Additionally, Sinninghe Damsté et al. (2012a) excluded sediments with GDGT-0/crenarchaeol ratios >2 on the basis that this ratio is always <2 in pure Thaumarchaeota cultures (Blaga et al., 2009; Sinninghe Damsté et al., 2012b), thereby avoiding instances when methanogens and archaea other than Thaumarchaeota must have contributed significantly to the isoGDGT pool. Our settling-particle data (Fig. 9B) suggest that this GDGT-0 threshold for Lake Chala must be shifted lower and exclude horizons with GDGT-0/crenarchaeol values > 0.7. Although the concentration and flux of GDGT-0 is not correlated to that of other isoGDGTs in Lake Chala, implying that the principal archaeal source of GDGT-0 contains no or limited amounts of other isoGDGTs and therefore does not directly affect TEX_{86}, a high GDGT-0/ crenarchaeol ratio is indirectly associated with reduced ecological niche for Thaumarchaeota.

Elevated amounts of GDGT-2 have been linked to production by non-thaumarchaeotal archaea (Pancost et al., 2001; Turich et al., 2007; Taylor et al., 2013), prompting Sinninghe Damsté et al. (2012a) to filter TEX_{86} data using a cut-off %GDGT-2 value of 45 (the percent contribution of GDGT-2 to the sum of GDGT-1,-2,-3, and cren'), as 45% is the proposed upper limit for marine sediments where the relationship between TEX_{86} and temperature was

originally observed (Kim et al., 2008). Additionally, it was later found that high relative abundances of GDGT-2 are related to deep-water-dwelling Thaumarchaeota (Villanueva et al., 2015; Kim et al., 2016; Besseling et al., 2019) and may also therefore alter the TEX_{86} signal produced in the surface waters. We found no relationship between cold-biased TEX_{86} temperature estimates and %GDGT-2 in our settling-particle data (Fig. 9D), probably because the majority of GDGT-2 production in Lake Chala occurs in the anoxic waters below the sediment trap depth or in the surface sediments (Sinninghe Damsté et al., 2012a). At the longer time scales considered in sediment records, the GDGT-2 cut-off value of 45% may still provide a useful indicator of deep water thaumarchaeotal isoGDGT production. Finally, although not explicitly considered by Sinninghe Damsté et al. (2012a), sediment horizons in the 25-kyr Lake Chala record with unrealistically low TEX_{86} values also had f[CREN'] values exceeding 0.05. Based on our settling-particle data (Fig. 9C) we propose to slightly lower the upper limit for f[CREN'] to 0.04. As discussed above, changes in Thaumarchaeotal communities have a direct impact on f[CREN'].

We recommend that the four criteria discussed above (BIT index, GDGT-0/crenarchaeol ratio, f[CREN'], and %GDGT-2) be used to filter out potentially unreliable TEX_{86} estimates. However, by applying this filtering method to the 25-kyr sediment record, the majority of the data points are excluded and only 38 out of 229 sediment horizons remain, all of them situated between ~14 and 24 ka (Fig. 8E). This method has clearly isolated several problematic sediments from the record. For example, it has excluded data from the early Holocene (11.5−10 ka) when temperature estimates are unexpectedly low, and also during the late Holocene when temperature estimates (well above 30 °C) are unrealistically high. In the remaining time slice, temperatures were coldest (~12.5 °C) between ~24 and 19 ka, coinciding with the timing of the LGM, and increased dramatically thereafter (up to ~27 °C). Although our adjusted filtering criteria resulted in the exclusion of several more data points in comparison to the published record of Sinninghe Damsté et al. (2012a), the questionably large temperature increase of nearly 15 °C from the last glacial into the Holocene still remains an issue. Even if the questionable three earliest data points (<~17 ka) of the filtered record (which fall within periods of generally higher %GDGT-2, BIT index, and GDGT-0/cren) are excluded, estimated deglacial temperature rise is over 7 °C. Paleo-temperature reconstructions from other east African lakes estimate a deglacial warming of ~2−4 °C (Powers et al., 2005; Tierney et al., 2008; Woltering et al., 2011; Bauersachs et al., 2021). It was previously speculated that the large magnitude of warming at Lake Chala may have been caused by a greater inflow of cold subsurface water into the lake or the influence of expansive ice caps atop Mt. Kilimanjaro on local climate during the LGM and Late Glacial periods (Sinninghe Damsté et al., 2012a). In light of our water-column studies in the modern system, it can also be suggested that the relationship between the niche of Thaumarchaeota production and the temperature gradient in the upper water column of Lake Chala may not have been stable over the substantial climate changes of the Late Glacial to Holocene transition. For this reason, even TEX_{86} temperature estimates during this interval which are deemed valid using our filtering criteria may not consistently represent mixed-layer temperature. Specifically, during the LGM and Late Glacial, relatively low air temperature and enhanced lake mixing likely caused depression of the oxycline and pushed the Thaumarchaeota niche to a deeper (colder) position, while the reverse is true of Holocene conditions, thus exacerbating the differences between TEX_{86} derived temperatures of the Last-Glacial period and the Holocene. These findings highlight the complexity of reliably estimating lake temperature using isoGDGTs and illustrates that in-depth functional investigation of the microbiota which produce the respective proxies in the modern lake systems, and filtering of sedimentary data are crucial to avoiding erroneous reconstruction of past climate regimes.

In Lake Chala, the ratios discussed above (BIT, f[CREN'], GDGT-0/cren) rely on relative changes in the size of the oxic versus the anoxic zones of the water column and particularly on the depth of the oxycline, which we found crucially impacted the growth of Thaumarchaeota. In lakes with similar dimensions and seasonal stratification patterns as Lake Chala, the above ratios may be investigated in the sedimentary record to flag certain intervals in the past where Thaumarchaeota production could be too low for TEX_{86} to accurately record temperature. However, in the absence of detailed water column studies this should be done with caution and where possible alongside other independent climate proxy data. Even amongst meromictic lakes there is a great diversity in the chemical characteristics at and below the oxic/anoxic boundary which likely impact the growth of these species and their niche distribution. In larger/deeper meromictic, lakes such as Lakes Malawi and Tanganyika (Kumar et al., 2019; Tierney et al., 2010), the shallowest position of the oxycline is deeper than ~150 m throughout the year, making it unlikely that Thaumarchaeota experience a dramatic disappearance caused by spatial restriction of their niche and/or photoinhibition; i.e. there is always a niche for Thaumarchaeota in the oxygenated mixed layer to thrive. Thus, there is greater potential for TEX_{86} to consistently predict past temperature variation in larger meromictic lakes. Previous research found that crenarchaeol is mostly absent or in low abundances in the surface sediments of small lakes, regardless that these lakes are generally fully or seasonally oxygenated (Powers et al., 2010). This suggests that conditions in most shallow lakes are not ideal for Thaumarchaeota, perhaps because shallower lake depth limits the establishment of different zonal niches of competing microbiota.

5. Conclusions

The principal isoGDGT compounds in the water column of Lake Chala are GDGT-0 and crenarchaeol, and they are produced by different groups of archaea. Thaumarchaeota are the main producers of all isoGDGTs except GDGT-0, and generally occur in the oxygenated uppermost water column. GDGT-0 production is highest in the permanently anoxic lower water column, and seasonally variable even though abiotic conditions at this depth are stable on this time scale. Although crenarchaeol production is only indirectly affected by rainfall, we propose that the BIT index measured in Lake Chala sediments is a reliable paleoprecipitation proxy because prolonged stratification of the upper water column under wet climatic conditions restricts Thaumarchaeota habitat, leading to low crenarchaeol fluxes and high BIT values. Overall, the influence of stratification on oxycline depth is key in understanding the archaeal ecology and production of isoGDGTs in Lake Chala, and explicitly considering this influence aids in the interpretation of sedimentary isoGDGT-proxy records. Past incidences of strong upper-water-column stratification can be recognized by high BIT-index values, high GDGT-0/crenarchaeol values, and a high proportion of the crenarchaeol isomer. Finally, TEX_{86}-based LST estimates are not reliable when strong stratification suppresses Group I.1a Thaumarchaeota. In Lake Chala, this is directly indicated by f[CREN'] values > 0.04 and indirectly by BIT-index values > 0.8 and isoGDGT/crenarchaeol ratio >0.7.

Research data

Research data is available via PANGAEA [https://doi.org/10.1594/PANGAEA.937241].

Author contributions for manuscript

Declaration of competing interest

The authors declare that they have no known competing financial interests or personal relationships that could have appeared to influence the work reported in this paper.

Acknowledgements

Appendix A. Supplementary data

Supplementary data to this article can be found online at https://doi.org/10.1016/j.quascirev.2021.107263.

References

Abdala Asbun, A., Besseling, M.A., Balzano, S., van Bleijswijk, J.D.L., Witte, H.J., Villanueva, L., Engelmann, J.C., 2020. Cascabel: a scalable and versatile amplicon sequence data analysis pipeline delivering reproducible and documented results. Front. Genet. 11. https://doi.org/10.3389/fgene.2020.489357.

Altschul, S.F., Gish, W., Miller, W., Myers, E.W., Lipman, D.J., 1990. Basic local alignment search tool. J. Mol. Biol. 215. https://doi.org/10.1016/S0022-2836(05)80360-2.

Andrews, S., 2010. FastQC - A Quality Control Tool for High Throughput Sequence Data. http://www.bioinformatics.babraham.ac.uk/projects/fastqc/ (Babraham Bioinformatics).

Bale, N.J., Sorokin, D.Y., Hopmans, E.C., Koenen, M., Irene Rijpstra, W.C., Villanueva, L., Wienk, H., Sinninghe Damsté, J.S., 2019a. New insights into the polar lipid composition of extremely halo(alkali)philic euryarchaea from hypersaline lakes. Front. Microbiol. 10. https://doi.org/10.3389/fmicb.2019.00377.

Bale, N.J., Palatinszky, M., Rijpstra, W.I.C., Herbold, C.W., Wagner, M., Damsté, J.S.S., 2019b. Membrane lipid composition of the moderately thermophilic ammonia-oxidizing archaeon "Candidatus Nitrosotenuis uzonensis" at different growth temperatures. Appl. Environ. Microbiol. 85. https://doi.org/10.1128/AEM.01332-19.

Bale, N.J., Irene Rijpstra, W.C., Sahonero-Canavesi, D.X., Oshkin, I.Y., Belova, S.E., Dedysh, S.N., Sinninghe Damsté, J.S., 2019c. Fatty acid and hopanoid adaption to cold in the methanotroph methylovulum psychrotolerans. Front. Microbiol. 10. https://doi.org/10.3389/fmicb.2019.00589.

Bale, N.J., Ding, S., Hopmans, E.C., Arts, M.G.I., Villanueva, L., Boschman, C., Haas, A.F., Schouten, S., Sinninghe Damsté, J.S., 2021. Lipidomics of environmental microbial communities. I: visualization of component distributions using untargeted analysis of high-resolution mass spectrometry data. Front. Microbiol. 12. https://doi.org/10.3389/fmicb.2021.659302.

Barker, P.A., Hurrell, E.R., Leng, M.J., Plessen, B., Wolff, C., Conley, D.J., Keppens, E., Milne, I., Cumming, B.F., Laird, K.R., Kendrick, C.P., Wynn, P.M., Verschuren, D., 2013. Carbon cycling within an East African lake revealed by the carbon isotope composition of diatom silica: a 25-ka record from Lake Challa, Mt. Kilimanjaro. Quat. Sci. Rev. 66. https://doi.org/10.1016/j.quascirev.2012.07.016.

Bauersachs, T., Russell, J.M., Evans, T.W., Schwalb, A., Schwark, L., 2021. A heterocyte glycolipid-based calibration to reconstruct past continental climate change. Nat. Commun. 12. https://doi.org/10.1038/s41467-021-22739-3.

Bechtel, A., Smittenberg, R.H., Bernasconi, S.M., Schubert, C.J., 2010. Distribution of branched and isoprenoid tetraether lipids in an oligotrophic and a eutrophic Swiss lake: insights into sources and GDGT-based proxies. Org. Geochem. 41. https://doi.org/10.1016/j.orggeochem.2010.04.022.

Berke, M.A., 2018. Reconstructing terrestrial paleoenvironments using sedimentary organic biomarkers. In: Vertebrate Paleobiology and Paleoanthropology. https://doi.org/10.1007/978-3-319-94265-0_8.

Besseling, M.A., Hopmans, E.C., Christine Boschman, R., Sinninghe Damsté, J.S., Villanueva, L., 2018. Benthic archaea as potential sources of tetraether membrane lipids in sediments across an oxygen minimum zone. Biogeosciences 15. https://doi.org/10.5194/bg-15-4047-2018.

Besseling, M.A., Hopmans, E.C., Koenen, M., van der Meer, M.T.J., Vreugdenhil, S., Schouten, S., Sinninghe Damsté, J.S., Villanueva, L., 2019. Depth-related differences in archaeal populations impact the isoprenoid tetraether lipid composition of the Mediterranean Sea water column. Org. Geochem. 135. https://doi.org/10.1016/j.orggeochem.2019.06.008.

Blaga, C.I., Reichart, G.J., Heiri, O., Sinninghe Damsté, J.S., 2009. Tetraether membrane lipid distributions in water-column particulate matter and sediments: a study of 47 European lakes along a north-south transect. J. Paleolimnol. 41. https://doi.org/10.1007/s10933-008-9242-2.

Blaga, C.I., Reichart, G.J., Vissers, E.W., Lotter, A.F., Anselmetti, F.S., Sinninghe Damsté, J.S., 2011. Seasonal changes in glycerol dialkyl glycerol tetraether concentrations and fluxes in a perialpine lake: implications for the use of the TEX_{86} and BIT proxies. Geochem. Cosmochim. Acta 75. https://doi.org/10.1016/j.gca.2011.08.016.

Blaga, C.I., Reichart, G.J., Lotter, A.F., Anselmetti, F.S., Sinninghe Damsté, J.S., 2013. A TEX_{86} lake record suggests simultaneous shifts in temperature in Central Europe and Greenland during the last deglaciation. Geophys. Res. Lett. 40. https://doi.org/10.1002/grl.50181.

Bligh, E.G., Dyer, W.J., 1959. A rapid method of total lipid extraction and purification. Can. J. Biochem. Physiol. 37. https://doi.org/10.1139/o59-099.

Bodé, S., de Wispelaere, L., Hemp, A., Verschuren, D., Boeckx, P., 2020. Water-isotope ecohydrology of mount kilimanjaro. Ecohydrology 13. https://doi.org/10.1002/eco.2171.

Buckles, L.K., Villanueva, L., Weijers, J.W.H., Verschuren, D., Damsté, J.S.S., 2013. Linking isoprenoidal GDGT membrane lipid distributions with gene abundances of ammonia-oxidizing Thaumarchaeota and uncultured crenarchaeotal groups in the water column of a tropical lake (Lake Challa, East Africa). Environ. Microbiol. 15, 2445−2462. https://doi.org/10.1111/1462-2920.12118.

Buckles, L.K., Weijers, J.W.H., Verschuren, D., Sinninghe Damsté, J.S., 2014. Sources of core and intact branched tetraether membrane lipids in the lacustrine environment: anatomy of Lake Challa and its catchment, equatorial East Africa. Geochem. Cosmochim. Acta 140, 106−126. https://doi.org/10.1016/j.gca.2014.04.042.

Buckles, L.K., Verschuren, D., Weijers, J.W.H., Cocquyt, C., Blaauw, M., Damsté, J.S.S., 2016. Interannual and (multi-)decadal variability in the sedimentary BIT index of Lake Challa, East Africa, over the past 2200 years: assessment of the precipitation proxy. Clim. Past 12, 1243−1262. https://doi.org/10.5194/cp-12-1243-2016.

Cao, M., Rivas-Ruiz, P., Trapote, M., del, C., Vegas-Vilarrúbia, T., Rull, V., Rosell-Melé, A., 2020. Seasonal effects of water temperature and dissolved oxygen on the isoGDGT proxy (TEX_{86}) in a Mediterranean oligotrophic lake. Chem. Geol. 551. https://doi.org/10.1016/j.chemgeo.2020.119759.

Caporaso, J.G., Kuczynski, J., Stombaugh, J., Bittinger, K., Bushman, F.D., Costello, E.K., Fierer, N., Pēa, A.G., Goodrich, J.K., Gordon, J.I., Huttley, G.A., Kelley, S.T., Knights, D., Koenig, J.E., Ley, R.E., Lozupone, C.A., McDonald, D., Muegge, B.D., Pirrung, M., Reeder, J., Sevinsky, J.R., Turnbaugh, P.J., Walters, W.A., Widmann, J., Yatsunenko, T., Zaneveld, J., Knight, R., 2010. QIIME allows analysis of high-throughput community sequencing data. Nat. Methods. https://doi.org/10.1038/nmeth.f.303.

Caporaso, J.G., Lauber, C.L., Walters, W.A., Berg-Lyons, D., Huntley, J., Fierer, N., Owens, S.M., Betley, J., Fraser, L., Bauer, M., Gormley, N., 2012. Ultra-high-throughput microbial community analysis on the Illumina HiSeq and MiSeq platforms. Int. Soc. Microb. Ecol. J. 6, 1621.

Castañeda, I.S., Schouten, S., 2011. A review of molecular organic proxies for examining modern and ancient lacustrine environments. Quat. Sci. Rev. https://doi.org/10.1016/j.quascirev.2011.07.009.

Coolen, M.J.L., Abbas, B., van Bleijswijk, J., Hopmans, E.C., Kuypers, M.M.M., Wakeham, S.G., Sinninghe Damsté, J.S., 2007. Putative ammonia-oxidizing Crenarchaeota in suboxic waters of the Black Sea: a basin-wide ecological study using 16S ribosomal and functional genes and membrane lipids. Environ. Microbiol. 9. https://doi.org/10.1111/j.1462-2920.2006.01227.x.

De Jonge, C., Hopmans, E.C., Zell, C.I., Kim, J.H., Schouten, S., Sinninghe Damsté, J.S., 2014. Occurrence and abundance of 6-methyl branched glycerol dialkyl glycerol tetraethers in soils: implications for palaeoclimate reconstruction. Geochem. Cosmochim. Acta. https://doi.org/10.1016/j.gca.2014.06.013.

De Rosa, M., Gambacorta, A., 1988. The Lipids of Archaebacteria. Progress in Lipid Research. https://doi.org/10.1016/0163-7827(88)90011-2.

Elling, F.J., Könneke, M., Nicol, G.W., Stieglmeier, M., Bayer, B., Spieck, E., de la Torre, J.R., Becker, K.W., Thomm, M., Prosser, J.I., Herndl, G.J., Schleper, C., Hinrichs, K.U., 2017. Chemotaxonomic characterisation of the thaumarchaeal lipidome. Environ. Microbiol. 19. https://doi.org/10.1111/1462-2920.13759.

Hemp, A., 2006. Continuum or zonation? Altitudinal gradients in the forest vegetation of Mt. Kilimanjaro. Plant Ecology 184. https://doi.org/10.1007/s11258-005-9049-4.

Holzheimer, M., Sinninghe Damsté, J.S., Schouten, S., Minnaard, A.J., 2021. Total synthesis of the alleged structure of crenarchaeol enables structure revision. Angew. Chem. Int. Ed. https://doi.org/10.1002/anie.202105384.

Hopmans, E.C., Weijers, J.W.H., Schefuß, E., Herfort, L., Sinninghe Damsté, J.S., Schouten, S., 2004. A novel proxy for terrestrial organic matter in sediments based on branched and isoprenoid tetraether lipids. Earth Planet Sci. Lett. 224, 107−116. https://doi.org/10.1016/j.epsl.2004.05.012.

Hopmans, E.C., Schouten, S., Sinninghe Damsté, J.S., 2016. The effect of improved chromatography on GDGT-based palaeoproxies. Org. Geochem. 93, 1−6. https://doi.org/10.1016/j.orggeochem.2015.12.006.

Huguet, C., Hopmans, E.C., Febo-Ayala, W., Thompson, D.H., Sinninghe Damsté, J.S., Schouten, S., 2006. An Improved Method to Determine the Absolute Abundance of Glycerol Dibiphytanyl Glycerol Tetraether Lipids. https://doi.org/10.1016/j.orggeochem.2006.05.008.

Huguet, C., Schimmelmann, A., Thunell, R., Lourens, L.J., Sinninghe Damsté, J.S., Schouten, S., 2007. A study of the TEX$_{86}$ paleothermometer in the water column and sediments of the Santa Barbara Basin, California. Paleoceanography 22. https://doi.org/10.1029/2006PA001310.

Kim, J.H., Schouten, S., Hopmans, E.C., Donner, B., Sinninghe Damsté, J.S., 2008. Global sediment core-top calibration of the TEX$_{86}$ paleothermometer in the ocean. Geochem. Cosmochim. Acta 72, 1154−1173. https://doi.org/10.1016/j.gca.2007.12.010.

Kim, J.H., van der Meer, J., Schouten, S., Helmke, P., Willmott, V., Sangiorgi, F., Koç, N., Hopmans, E.C., Damsté, J.S.S., 2010. New indices and calibrations derived from the distribution of crenarchaeal isoprenoid tetraether lipids: implications for past sea surface temperature reconstructions. Geochem. Cosmochim. Acta 74, 4639−4654. https://doi.org/10.1016/j.gca.2010.05.027.

Kim, J.G., Jung, M.Y., Park, S.J., Rijpstra, W.I.C., Sinninghe Damsté, J.S., Madsen, E.L., Min, D., Kim, J.S., Kim, G.J., Rhee, S.K., 2012. Cultivation of a highly enriched ammonia-oxidizing archaeon of thaumarchaeotal group I.1b from an agricultural soil. Environ. Microbiol. 14. https://doi.org/10.1111/j.1462-2920.2012.02740.x.

Kim, J.H., Villanueva, L., Zell, C., Sinninghe Damsté, J.S., 2016. Biological source and provenance of deep-water derived isoprenoid tetraether lipids along the Portuguese continental margin. Geochem. Cosmochim. Acta 172. https://doi.org/10.1016/j.gca.2015.09.010.

Koga, Y., Akagawa-Matsushita, M., Ohga, M., Nishihara, M., 1993. Taxonomic significance of the distribution of component parts of polar ether lipids in methanogens. Syst. Appl. Microbiol. 16. https://doi.org/10.1016/S0723-2020(11)80264-X.

Kubo, K., Lloyd, K.G., F Biddle, J., Amann, R., Teske, A., Knittel, K., 2012. Archaea of the Miscellaneous Crenarchaeotal Group are abundant, diverse and widespread in marine sediments. ISME J. 6. https://doi.org/10.1038/ismej.2012.37.

Kumar, D.M., Woltering, M., Hopmans, E.C., Sinninghe Damsté, J.S., Schouten, S., Werne, J.P., 2019. The vertical distribution of Thaumarchaeota in the water column of Lake Malawi inferred from core and intact polar tetraether lipids. Org. Geochem. https://doi.org/10.1016/j.orggeochem.2019.03.004.

Lavergne, C., Hugoni, M., Dupuy, C., Agogué, H., 2018. First evidence of the presence and activity of archaeal C3 group members in an Atlantic intertidal mudflat. Sci. Rep. 8. https://doi.org/10.1038/s41598-018-30222-1.

Meador, T.B., Bowles, M., Lazar, C.S., Zhu, C., Teske, A., Hinrichs, K.U., 2015. The archaeal lipidome in estuarine sediment dominated by members of the Miscellaneous Crenarchaeotal Group. Environ. Microbiol. 17. https://doi.org/10.1111/1462-2920.12716.

Merbt, S.N., Stahl, D.A., Casamayor, E.O., Martí, E., Nicol, G.W., Prosser, J.I., 2012. Differential photoinhibition of bacterial and archaeal ammonia oxidation. FEMS (Fed. Eur. Microbiol. Soc.) Microbiol. Lett. 327. https://doi.org/10.1111/j.1574-6968.2011.02457.x.

Moernaut, J., Verschuren, D., Charlet, F., Kristen, I., Fagot, M., de Batist, M., 2010. The seismic-stratigraphic record of lake-level fluctuations in Lake Challa:

hydrological stability and change in equatorial East Africa over the last 140 kyr. Earth Planet Sci. Lett. 290. https://doi.org/10.1016/j.epsl.2009.12.023.

Nankabirwa, A., de Crop, W., van der Meeren, T., Cocquyt, C., Plisnier, P.D., Balirwa, J., Verschuren, D., 2019. Phytoplankton communities in the crater lakes of western Uganda, and their indicator species in relation to lake trophic status. Ecol. Indicat. 107. https://doi.org/10.1016/j.ecolind.2019.105563.

Pancost, R.D., Hopmans, E.C., Sinninghe Damsté, J.S., 2001. Archaeal lipids in mediterranean cold seeps: molecular proxies for anaerobic methane oxidation. Geochem. Cosmochim. Acta 65. https://doi.org/10.1016/S0016-7037(00)00562-7.

Payne, B.R., 1970. Water balance of Lake Chala and its relation to groundwater from tritium and stable isotope data. J. Hydrol. 11. https://doi.org/10.1016/0022-1694(70)90114-9.

Pester, M., Schleper, C., Wagner, M., 2011. The Thaumarchaeota: an emerging view of their phylogeny and ecophysiology. Curr. Opin. Microbiol. 14. https://doi.org/10.1016/j.mib.2011.04.007.

Pitcher, A., Rychlik, N., Hopmans, E.C., Spieck, E., Rijpstra, W.I.C., Ossebaar, J., Schouten, S., Wagner, M., Damsté, J.S.S., 2010. Crenarchaeol dominates the membrane lipids of Candidatus Nitrososphaera gargensis, a thermophilic Group I.1b Archaeon. ISME J. 4. https://doi.org/10.1038/ismej.2009.138.

Pitcher, A., Hopmans, E.C., Mosier, A.C., Park, S.J., Rhee, S.K., Francis, C.A., Schouten, S., Sinninghe Damsté, J.S., 2011. Core and intact polar glycerol dibiphytanyl glycerol tetraether lipids of ammonia-oxidizing Archaea enriched from marine and estuarine sediments. Appl. Environ. Microbiol. 77. https://doi.org/10.1128/AEM.02758-10.

Powers, L.A., Johnson, T.C., Werne, J.P., Castañeda, I.S., Hopmans, E.C., Sinninghe Damsté, J.S., Schouten, S., 2005. Large temperature variability in the southern african tropics since the last glacial maximum. Geophys. Res. Lett. 32. https://doi.org/10.1029/2004GL022014.

Powers, L., Werne, J.P., Vanderwoude, A.J., Sinninghe Damsté, J.S., Hopmans, E.C., Schouten, S., 2010. Applicability and calibration of the TEX$_{86}$ paleothermometer in lakes. Org. Geochem. 41, 404−413. https://doi.org/10.1016/j.orggeochem.2009.11.009.

Powers, L.A., Johnson, T.C., Werne, J.P., Castañeda, I.S., Hopmans, E.C., Sinninghe Damsté, J.S., Schouten, S., 2011. Organic geochemical records of environmental variability in Lake Malawi during the last 700 years, Part I: the TEX$_{86}$ temperature record. Palaeogeogr. Palaeoclimatol. Palaeoecol. 303. https://doi.org/10.1016/j.palaeo.2010.09.006.

Rossel, P.E., Lipp, J.S., Fredricks, H.F., Arnds, J., Boetius, A., Elvert, M., Hinrichs, K.U., 2008. Intact polar lipids of anaerobic methanotrophic archaea and associated bacteria. Org. Geochem. 39. https://doi.org/10.1016/j.orggeochem.2008.02.021.

Rossel, P.E., Elvert, M., Ramette, A., Boetius, A., Hinrichs, K.U., 2011. Factors controlling the distribution of anaerobic methanotrophic communities in marine environments: evidence from intact polar membrane lipids. Geochem. Cosmochim. Acta 75. https://doi.org/10.1016/j.gca.2010.09.031.

Schouten, S., Wakeham, S.G., Damsté, J.S.S., 2001. Evidence for anaerobic methane oxidation by archaea in euxinic waters of the Black Sea. In: Organic Geochemistry. https://doi.org/10.1016/S0146-6380(01)00110-3.

Schouten, S., Hopmans, E.C., Schefuß, E., Sinninghe Damsté, J.S., 2002. Distributional variations in marine crenarchaeotal membrane lipids: a new tool for reconstructing ancient sea water temperatures? Earth Planet Sci. Lett. 204, 265−274. https://doi.org/10.1016/S0012-821X(02)00979-2.

Schouten, S., Hopmans, E.C., Sinninghe Damsté, J.S., 2013. The organic geochemistry of glycerol dialkyl glycerol tetraether lipids: a review. Org. Geochem. 54, 19−61. https://doi.org/10.1016/j.orggeochem.2012.09.006.

Schubotz, F., Lipp, J.S., Elvert, M., Hinrichs, K.U., 2011. Stable carbon isotopic compositions of intact polar lipids reveal complex carbon flow patterns among hydrocarbon degrading microbial communities at the Chapopote asphalt volcano. Geochem. Cosmochim. Acta 75. https://doi.org/10.1016/j.gca.2011.05.018.

Sinninghe Damsté, J.S., Schouten, S., Hopmans, E.C., van Duin, A.C.T., Geenevasen, J.A.J., 2002. Crenarchaeol: the characteristic core glycerol dibiphytanyl glycerol tetraether membrane lipid of cosmopolitan pelagic crenarchaeota. JLR (J. Lipid Res.) 43. https://doi.org/10.1194/jlr.M200148-JLR200.

Sinninghe Damsté, J.S., Ossebaar, J., Abbas, B., Schouten, S., Verschuren, D., 2009. Fluxes and distribution of tetraether lipids in an equatorial African lake: constraints on the application of the TEX$_{86}$ palaeothermometer and BIT index in lacustrine settings. Geochem. Cosmochim. Acta 73, 4232−4249. https://doi.org/10.1016/j.gca.2009.04.022.

Sinninghe Damsté, J.S., Ossebaar, J., Schouten, S., Verschuren, D., 2012a. Distribution of tetraether lipids in the 25-ka sedimentary record of Lake Challa: extracting reliable TEX 86 and MBT/CBT palaeotemperatures from an equatorial African lake. Quat. Sci. Rev. 50, 43−54. https://doi.org/10.1016/j.quascirev.2012.07.001.

Sinninghe Damsté, J.S., Rijpstra, W.I.C., Hopmans, E.C., Jung, M.Y., Kim, J.G., Rhee, S.K., Stieglmeier, M., Schleper, C., 2012b. Intact polar and core glycerol dibiphytanyl glycerol tetraether lipids of group I.1a and I.1b Thaumarchaeota in soil. Appl. Environ. Microbiol. 78. https://doi.org/10.1128/AEM.01681-12.

Sinninghe Damsté, J.S., Rijpstra, W.I.C., Hopmans, E.C., den Uijl, M.J., Weijers, J.W.H., Schouten, S., 2018. The enigmatic structure of the crenarchaeol isomer. Org. Geochem. 124. https://doi.org/10.1016/j.orggeochem.2018.06.005.

Sollai, M., Villanueva, L., Hopmans, E.C., Reichart, G.J., Sinninghe Damsté, J.S., 2019. A combined lipidomic and 16S rRNA gene amplicon sequencing approach reveals archaeal sources of intact polar lipids in the stratified Black Sea water column. Geobiology 17. https://doi.org/10.1111/gbi.12316.

Strapoc, D., Picardal, F.W., Turich, C., Schaperdoth, I., Macalady, J.L., Lipp, J.S., Lin, Y.S., Ertefai, T.F., Schubotz, F., Hinrichs, K.U., Mastalerz, M., Schimmelmann, A., 2008.

Methane-producing microbial community in a coal bed of the Illinois Basin. Appl. Environ. Microbiol. 74. https://doi.org/10.1128/AEM.02341-07.

Sun, W., Zhang, E., Chang, J., Shulmeister, J., I Bird, M., Zhao, C., Jiang, Q., Shen, J., 2020. Archaeal lipid-inferred paleohydrology and paleotemperature of Lake Chenghai during the Pleistocene-Holocene transition. Clim. Past 16. https://doi.org/10.5194/cp-16-833-2020.

Taylor, K.W.R., Huber, M., Hollis, C.J., Hernandez-Sanchez, M.T., Pancost, R.D., 2013. Re-evaluating modern and Palaeogene GDGT distributions: implications for SST reconstructions. Global Planet. Change. https://doi.org/10.1016/j.gloplacha.2013.06.011.

Tierney, J.E., Russell, J.M., Huang, Y., Sinninghe Damsté, J.S., Hopmans, E.C., Cohen, A.S., 2008. Northern hemisphere controls on tropical southeast African climate during the past 60,000 years. Science 322. https://doi.org/10.1126/science.1160485.

Tierney, J.E., Mayes, M.T., Meyer, N., Johnson, C., Swarzenski, P.W., Cohen, A.S., Russell, J.M., 2010. Late-twentieth-century warming in lake Tanganyika unprecedented since AD 500. Nat. Geosci. 3, 422–425. https://doi.org/10.1038/ngeo865.

Tierney, J.E., Schouten, S., Pitcher, A., Hopmans, E.C., Sinninghe Damsté, J.S., 2012. Core and intact polar glycerol dialkyl glycerol tetraethers (GDGTs) in Sand Pond, Warwick, Rhode Island (USA): insights into the origin of lacustrine GDGTs. Geochem. Cosmochim. Acta 77. https://doi.org/10.1016/j.gca.2011.10.018.

Turich, C., Freeman, K.H., Bruns, M.A., Conte, M., Jones, A.D., Wakeham, S.G., 2007. Lipids of marine Archaea: patterns and provenance in the water-column and sediments. Geochem. Cosmochim. Acta 71. https://doi.org/10.1016/j.gca.2007.04.013.

van Bree, L.G.J., Peterse, F., van der Meer, M.T.J., Middelburg, J.J., Negash, A.M.D., de Crop, W., Cocquyt, C., Wieringa, J.J., Verschuren, D., Sinninghe Damsté, J.S., 2018. Seasonal variability in the abundance and stable carbon-isotopic composition of lipid biomarkers in suspended particulate matter from a stratified equatorial lake (Lake Chala, Kenya/Tanzania): implications for the sedimentary record. Quat. Sci. Rev. https://doi.org/10.1016/j.quascirev.2018.05.023.

van Bree, L.G.J., Peterse, F., Baxter, A.J., de Crop, W., van Grinsven, S., Villanueva, L., Verschuren, D., Sinninghe Damsté, J.S., 2020. Seasonal variability and sources of in situ brGDGT production in a permanently stratified African crater lake. Biogeosciences 17. https://doi.org/10.5194/bg-17-5443-2020.

Verschuren, D., Sinninghe Damsté, J.S., Moernaut, J., Kristen, I., Blaauw, M., Fagot, M., Haug, G.H., 2009. Half-precessional dynamics of monsoon rainfall near the East African Equator. Nature 462, 637–641. https://doi.org/10.1038/nature08520.

Villanueva, L., Schouten, S., Sinninghe Damsté, J.S., 2015. Depth-related distribution of a key gene of the tetraether lipid biosynthetic pathway in marine Thaumarchaeota. Environ. Microbiol. 17. https://doi.org/10.1111/1462-2920.12508.

Wang, H., Liu, W., Zhang, C.L., Wang, Z., Wang, J., Liu, Z., Dong, H., 2012. Distribution of glycerol dialkyl glycerol tetraethers in surface sediments of Lake Qinghai and surrounding soil. Org. Geochem. 47. https://doi.org/10.1016/j.orggeochem.2012.03.008.

Wang, H.Y., Dong, H.L., Zhang, C.L., Jiang, H.C., Liu, W.G., 2016. A 12-kyr record of microbial branched and isoprenoid tetraether index in Lake Qinghai, northeastern Qinghai-Tibet Plateau: implications for paleoclimate reconstruction. Sci. China Earth Sci. https://doi.org/10.1007/s11430-015-5213-4.

Weber, Y., de Jonge, C., Rijpstra, W.I.C., Hopmans, E.C., Stadnitskaia, A., Schubert, C.J., Lehmann, M.F., Sinninghe Damsté, J.S., Niemann, H., 2015. Identification and carbon isotope composition of a novel branched GDGT isomer in lake sediments: evidence for lacustrine branched GDGT production. Geochem. Cosmochim. Acta 154, 118–129. https://doi.org/10.1016/j.gca.2015.01.032.

Weber, Y., Sinninghe Damsté, J.S., Hopmans, E.C., Lehmann, M.F., Niemann, H., 2017. Incomplete recovery of intact polar glycerol dialkyl glycerol tetraethers from lacustrine suspended biomass. Limnol Oceanogr. Methods 15. https://doi.org/10.1002/lom3.10198\.

Weber, Y., Sinninghe Damsté, J.S., Zopfi, J., de Jonge, C., Gilli, A., Schubert, C.J., Lepori, F., Lehmann, MoritzF., Niemann, H., 2018. Redox-dependent niche differentiation of tetraether producing bacteria: evidence for multiple branched GDGT sources in lakes. In: Proceedings of the National Academy of Sciences of the United States of America. https://doi.org/10.1073/pnas.1805186115.

Weijers, J.W.H., Schouten, S., Hopmans, E.C., Geenevasen, J.A.J., David, O.R.P., Coleman, J.M., Pancost, R.D., Sinninghe Damsté, J.S., 2006. Membrane lipids of mesophilic anaerobic bacteria thriving in peats have typical archaeal traits. Environ. Microbiol. 8. https://doi.org/10.1111/j.1462-2920.2005.00941.x.

Weijers, J.W.H., Schouten, S., van den Donker, J.C., Hopmans, E.C., Sinninghe Damsté, J.S., 2007. Environmental controls on bacterial tetraether membrane lipid distribution in soils. Geochem. Cosmochim. Acta 71. https://doi.org/10.1016/j.gca.2006.10.003.

Wolff, C., Haug, G.H., Timmermann, A., Sinninghe Damsté, J.S., Brauer, A., Sigman, D.M., Cane, M.A., Verschuren, D., 2011. Reduced interannual rainfall variability in East Africa during the last ice age. Science 333. https://doi.org/10.1126/science.1203724.

Wolff, C., Kristen-Jenny, I., Schettler, G., Plessen, B., Meyer, H., Dulski, P., Naumann, R., Brauer, A., Verschuren, D., Haug, G.H., 2014. Modern seasonality in Lake Challa (Kenya/Tanzania) and its sedimentary documentation in recent lake sediments. Limnol. Oceanogr. 59. https://doi.org/10.4319/lo.2014.59.5.1621.

Woltering, M., Johnson, T.C., Werne, J.P., Schouten, S., Sinninghe Damsté, J.S., 2011. Late pleistocene temperature history of southeast Africa: a TEX$_{86}$ temperature record from Lake Malawi. Palaeogeogr. Palaeoclimatol. Palaeoecol. 303. https://doi.org/10.1016/j.palaeo.2010.02.013.

Woltering, M., Werne, J.P., Kish, J.L., Hicks, R., Sinninghe Damsté, J.S., Schouten, S., 2012. Vertical and temporal variability in concentration and distribution of thaumarchaeotal tetraether lipids in Lake Superior and the implications for the application of the TEX$_{86}$ temperature proxy. Geochem. Cosmochim. Acta. https://doi.org/10.1016/j.gca.2012.03.024.

Wörmer, L., Lipp, J.S., Schröder, J.M., Hinrichs, K.U., 2013. Application of two new LC-ESI-MS methods for improved detection of intact polar lipids (IPLs) in environmental samples. Org. Geochem. 59. https://doi.org/10.1016/j.orggeochem.2013.03.004.

Wu, J., Yang, H., Pancost, R.D., Naafs, B.D.A., Qian, S., Dang, X., Sun, H., Pei, H., Wang, R., Zhao, S., Xie, S., 2021. Variations in dissolved O$_2$ in a Chinese lake drive changes in microbial communities and impact sedimentary GDGT distributions. Chem. Geol. 579. https://doi.org/10.1016/j.chemgeo.2021.120348.

Yoshinaga, M.Y., Kellermann, M.Y., Rossel, P.E., Schubotz, F., Lipp, J.S., Hinrichs, K.U., 2011. Systematic fragmentation patterns of archaeal intact polar lipids by high-performance liquid chromatography/electrospray ionization ion-trap mass spectrometry. Rapid Commun. Mass Spectrom. 25. https://doi.org/10.1002/rcm.5251.

Zhang, J., Kobert, K., Flouri, T., Stamatakis, A., 2014. PEAR: a fast and accurate Illumina Paired-End reAd mergeR. Bioinformatics 30. https://doi.org/10.1093/bioinformatics/btt593.

Zhang, Z., Smittenberg, R.H., Bradley, R.S., 2016. GDGT distribution in a stratified lake and implications for the application of TEX$_{86}$ in paleoenvironmental reconstructions. Sci. Rep. 6. https://doi.org/10.1038/srep34465.

Zhou, Z., Pan, J., Wang, F., Gu, J.D., Li, M., 2018. Bathyarchaeota: globally distributed metabolic generalists in anoxic environments. FEMS (Fed. Eur. Microbiol. Soc.) Microbiol. Rev. https://doi.org/10.1093/femsre/fuy023.